BIOLOGICAL EFFECTS OF ACOUSTIC CAVITATION

THE UNIVERSITY OF MISSISSIPPI
PHYSICAL ACOUSTICS RESEARCH GROUP
DEPARTMENT OF PHYSICS AND ASTRONOMY

Approved for Public Release: Distribution Unlimited

Technical Report for
Office of Naval Research
Contract N00014-84-C-0193

BIOLOGICAL EFFECTS
OF
ACOUSTIC CAVITATION

by

Lawrence A. Crum
Physical Acoustics Research Laboratory
Department of Physics and Astronomy
The University of Mississippi
University, MS 38677

June 15, 1985

Unclassified

SECURITY CLASSIFICATION OF THIS PAGE (When Data Entered)

REPORT DOCUMENTATION PAGE		READ INSTRUCTIONS BEFORE COMPLETING FORM
1. REPORT NUMBER 3-85	2. GOVT ACCESSION NO. A157513	3. RECIPIENT'S CATALOG NUMBER
4. TITLE (and Subtitle) Biological Effects of Acoustic Cavitation		5. TYPE OF REPORT & PERIOD COVERED Technical 6. PERFORMING ORG. REPORT NUMBER
7. AUTHOR(s) Lawrence A. Crum		8. CONTRACT OR GRANT NUMBER(s) N00014-84-C-0193
9. PERFORMING ORGANIZATION NAME AND ADDRESS Physical Acoustics Research Laboratory Department of Physics and Astronomy The University of MS., University, MS 38677		10. PROGRAM ELEMENT, PROJECT, TASK AREA & WORK UNIT NUMBERS
11. CONTROLLING OFFICE NAME AND ADDRESS		12. REPORT DATE June 15, 1985 13. NUMBER OF PAGES 94
14. MONITORING AGENCY NAME & ADDRESS(if different from Controlling Office)		15. SECURITY CLASS. (of this report) Unclassified 15a. DECLASSIFICATION/DOWNGRADING SCHEDULE

16. DISTRIBUTION STATEMENT (of this Report)

Approved for Public Release: Distribution Unlimited

17. DISTRIBUTION STATEMENT (of the abstract entered in Block 20, if different from Report)

18. SUPPLEMENTARY NOTES

19. KEY WORDS (Continue on reverse side if necessary and identify by block number)

Cavitation,
Biological Effects,
Bubbles,
Nucleation,
Nonlinear Oscillation,
Rectified Diffusion.

20. ABSTRACT (Continue on reverse side if necessary and identify by block number)

This report contains the lecture notes of the author for a short course entitled "Biological Effects of Acoustic Cavitation" presented at the University of Rochester, May 13-16, 1985. Lecture notes pertain to:

Cont'd p4

DD FORM 1 JAN 73 1473 EDITION OF 1 NOV 65 IS OBSOLETE
S/N 0102-LF-014-6601

Unclassified
SECURITY CLASSIFICATION OF THIS PAGE (When Data Entered)

BIOLOGICAL EFFECTS
OF
ACOUSTIC CAVITATION

Lecture 2

Contld

Nucleation, rectified diffusion, stable cavitation and experimental measurements. Contents of lecture & notes included.

Contd p iii

by

Lawrence A. Crum

Physical Acoustics Research Group
Department of Physics and Astronomy
The University of Mississippi
University, MS 38677

LECTURE NO. 2

LAWRENCE A. CRUM

TABLE OF CONTENTS

I. Stabilization and Nucleation of Cavitation Nuclei

It is rather well known that liquids possess a tensile strength several orders of magnitude less than predicted due to the presence of inhomogeneities suspended in the bulk of the liquid. These preferential sites for liquid rupture are commonly called nuclei and are presumed to be small pockets of undissolved gas. The fact that experiments [1] involving small samples of liquids that do not possess nuclei gives values of the tensile strength close to the value predicted by theory indicates rather conclusively that these nuclei do exist and essentially determine the experimental tensile strength of liquids.

Before we consider the various models that have been suggested as possible candidates for cavitation nuclei, it is important to keep fresh in our minds a rather remarkable fact concerning transient cavitation - no matter where one makes the measurement (in a geographical sense), one finds that there exists a rather sharply defined threshold acoustic pressure below which cavitation rarely occurs. (A similar threshold exists for many aspects of stable cavitation, although it is not so sharply observed). For example, consider Fig. 1 which shows some raw data [2] taken from a measurement of the acoustic cavitation threshold of water. Using an objective detection criterion, i.e., the detection of a sonoluminescence pulse of a predetermined minimum height, all 30 measurements taken over a period of 2 hours gave peak acoustic threshold pressures within a range of a db or so. We shall have to conclude that the "inhomogeneities are rather homogeneous".

Having accepted the experimental fact that nuclei exist, and are essentially pockets of gas, we can quickly discover that they must be both

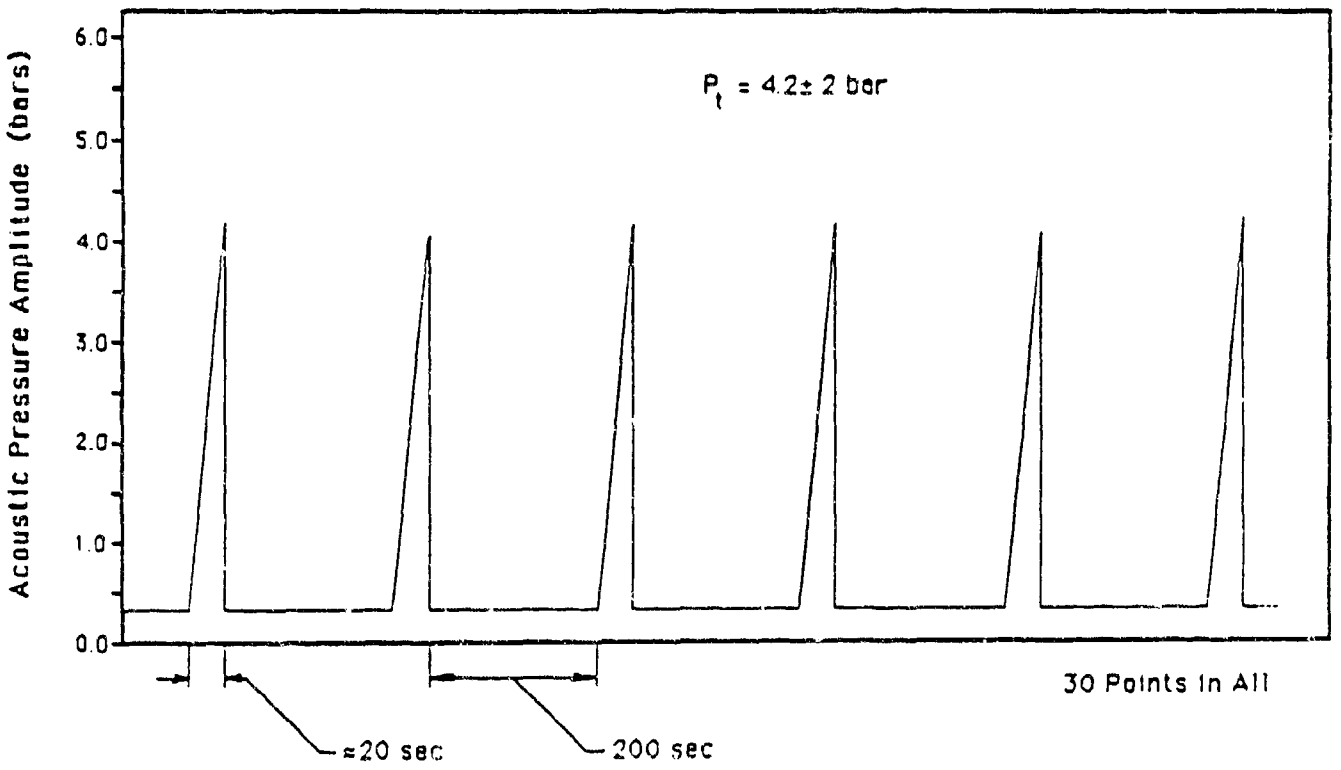

Fig. 1. Strip chart record of acoustic cavitation threshold measurements in distilled water at a frequency of 69 kHz. The water was saturated with gas. The figure shows that as the pressure amplitude (vertical axis) was increased linearly with time, the cavitation inception point is well defined and stable.

complex and simple at the same time. Complex because there must exist some stabilization mechanism to prevent the gas from dissolving (and we shall see that this effect requires some pretty sophisticated models), and simple because these nuclei must be the same throughout a liquid taken from around the world. We shall now consider the various mechanisms that would permit a pocket of gas to exist for indefinite periods of time in a liquid - in essence, to be stabilized against dissolution. First a bit of terminology: pockets of gas, no matter what geometrical shape, are to be called nuclei; the prevention of this gas from dissolving is called stabilization; the release of this gas from its stabilized condition so that it can grow into an observable event is called nucleation; the event itself is called cavitation.

A. Free bubbles

It is by now well known that free gas bubbles present in a liquid will either rise to the surface or quickly dissolve due to the "Laplace pressure" exerted by surface tension. The stability of free gas bubbles has been discussed by numerous authors; see references [3-5] to consider a few. An example or two can give us some applicable numbers. A gas bubble of radius 100 μm would take 6900 seconds to dissolve but would rise through water at an approximate terminal velocity of 2 cm/sec; a bubble of 1.0 μm would not rise significantly (due to Brownian motion) but would dissolve within 60 ms if it were in water. Biological media present a different environment than distilled water, but it is reasonable to assume that large bubbles are extremely rare and surface tension forces, though smaller than those for pure water would still force small bubbles to dissolve. (The argument that local gas supersaturation could balance the Laplace pressure can be countered by noting that the Laplace pressure for a 1.0 μm bubble is over an atmosphere - such levels of supersaturation would be extremely

rare.)

B. Ionic charges

Akulichev [6] has suggested that free ions present in a liquid could stabilize a pocket of gas by Coulomb repulsion. He has presented supporting evidence that indicates that the concentration of certain hydrophobic ions can significantly affect the cavitation threshold of aqueous solutions. We have examined this model also and can verify that the acoustic cavitation threshold is significantly affected by the dissolved ion concentration. For example, consider Fig. 2, which shows the influence of the cavitation threshold on the concentration of the salt KI. (We have extended the range of the ion concentration nearly two orders of magnitude lower than Akulichev.) Unfortunately, it is still not possible to present a viable model detailing the physical mechanisms that leads to nuclei stabilization. At best, we can say that the presence of dissolved ions can significantly influence the cavitation threshold, and that this fact should be kept in mind when dealing with this concept.

C. Organic skins

A polar liquid such as water is known to rapidly acquire trace amounts of organic solutes that are surface-active. Fox and Herzfeld [7] suggested a model for cavitation nuclei based on these organic molecules. In their view, a rigid skin of these organic molecules would form about a dissolving bubble preventing the bubble from dissolving further and thus stabilizing the nucleus. For future contrast with a model to be discussed below, note that in this model the skin is assumed to be rigid. Unfortunately for this model, the experiments of Strasberg [8] who considered the cavitation threshold as a function of applied static pressure, seriously challenged its veracity. If the nucleus is truly surrounded with a rigid skin, there would exist a crushing pressure whereby the nucleus would be destroyed and

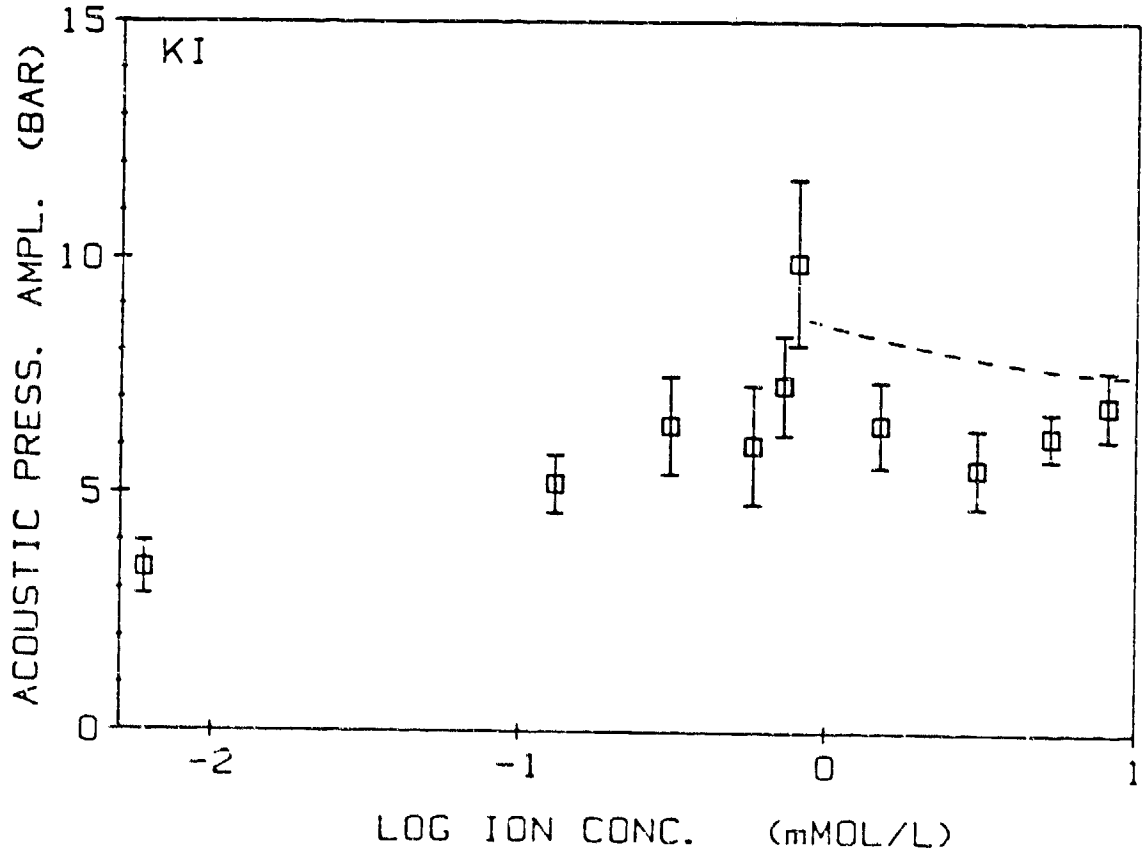

Fig. 2. Variation of the acoustic cavitation threshold of distilled water with concentration of KI. The frequency was 69 kHz and the dissolved gas concentration was 30% of saturation. The dashed line shows the previous results of Aculichev [6] that were made at a lower gas concentration.

the threshold would approach the theoretical limit. Strasberg's measurements which indicated a monotonic increase in threshold with applied static pressure, rather than a sharp discontinuity, prompted even Herzfeld to subsequently reject the model [9].

A modified Herzfeld-Fox model was then introduced by Sirotyuk [10] who gave few details but argued that surface active molecules could stabilize a gas bubble from dissolution. The experimental evidence given by Sirotyuk in support of the model is, in the view of the author, considerably flawed. However, there is probably considerable merit in the model, as properly modified by Yount.

Yount [11-15] has developed the surface active agent concept into a detailed and sophisticated model that explains a considerable volume of data obtained from studies of bubble formation in supersaturated gelatine. Since this model appears to have experimental support, and since it seems to have a specific applicability to situations involving organic solutions, it is appropriate to consider this model in more detail when considering nucleation in biological systems. (An excellent and detailed review of this model has been accomplished by Atchley [16] ; much of the following discussion is taken from this dissertation.)

This model is called by Yount the "Varying Permeability" model as will be obvious from the following discussion. In contrast to Herzfeld-Fox and following Sirotyuk, it is assumed that the dissolution of gas bubbles is halted by a non-rigid organic skin. This skin has mechanical strength against compression, but none against tension. This postulated nucleus is depicted schematically in figure 3.

The nucleus is formed in the following manner. A gas bubble is introduced into a liquid by some mechanism that is not important at the moment,

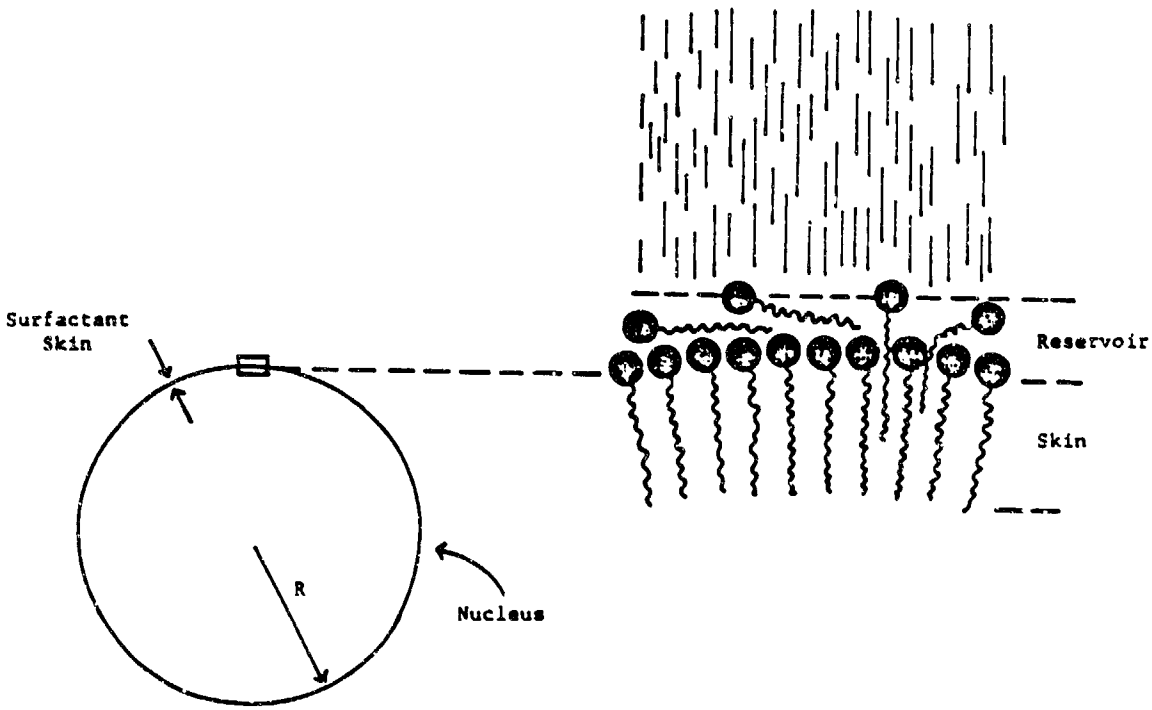

Fig. 3. A model of microbubble stabilization based upon the variable-permeability concept of Yount [11].

and begins to dissolve. While the dissolution takes place, surface active molecules accummulate on the surface. Eventually, within minutes or seconds, the density of these surfactants is such that they resist the collapse of the bubble. This is presumably a Coulomb interaction. These molecules are polar (or perhaps even carry a net charge) and align themselves such that their polar "heads" face outward (toward the water) and their tails (typically hydrocarbons) stick inward. Thus, as the density increases, the separation of the heads becomes small enough for dipole fields to become important. Of course, one would expect that if the surfactants were charged, the density at which stabilization occurs would be lower because monopolar fields vary as r^{-2} rather than r^{-3}.

Once the critical density is reached, the radius of the nucleus may vary through changes in the number of molecules on the skin. The equilibrium condition for this nucleus is that the electrochemical potentials of the skin and the reservoir must be equal. The reservoir is a thin (perhaps monomolecular) layer of non-aligned surfactants which surrounds the skin of aligned molecules. This equilibrium condition can be satisfied by the accretion or deletion of molecules from the skin (or reservoir), resulting in a "large-scale" change in radius. Having adjusted the radius in this manner, subsequent "small-scale" changes in radius occur. These changes involve only the adjustment of the separation of adjacent skin molecules, not a change in the number of molecules. At equilibrium, the nucleus can be thought of as two concentric shells of negligible thickness--the outer one, the reservoir, is in contact with the liquid and the inner one, the skin, is in contact with the gas. So far, this model has only been used to make predictions about compression/decompression processes during which gas diffusion can play a major role and which is basically a quasistatic process. However, Yount [14] has calculated characteristic times in which a

skin molecule can be accreted or deleted, due to an inequality of electrochemical potentials, and found them to range from 10^{-3} to 10^{-6} seconds. The shortest times approach the period of acoustic signals used in ultrasonic studies. This would imply that large-scale changes in radius may be able to keep up with the variations in applied pressure associated with acoustic cavitation.

As mentioned above, Yount has performed only long time-scale experiments. A typical experiment will now be described. During the experiment, gelatin samples (surface tension around 50-55 dyn/cm) are subjected to a pressure schedule which involves a compression, a resting time for equilibrium to occur, and a subsequent rapid decompression. The sample, about 0.4 ml in volume, initially at a pressure P_o, is rapidly compressed to a pressure P_m. "Rapidly" means that no gas diffuses out of the nucleus during the compression. The sample is held at P_m long enough for the dissolved gas pressure in the sample to come to equilibrium at P_m; i.e., it becomes saturated. The holding time is typically 5.25 hours. The ambient pressure is then reduced rapidly to P_f resulting in the growth of some of the nuclei. This growth occurs through gas diffusion from the now supersaturated liquid into the nuclei. Several minutes are allowed for the nuclei to grow to visible size. Then the total number of visible bubbles are counted and correlated with the pressure schedule. Yount defines the crushing pressure, P_{crush}, as $P_m - P_o$; and the supersaturation pressure, P_{ss}, as $P_m - P_f$. One manner of data presentation is a graph of P_{ss} vs. P_{crush} for lines of constant number of bubbles. Such a graph is reproduced in figure 4.

The isopleths (lines of constant number of bubbles) in figure 4 show a gradual decrease in slope at $P_{crush} = P^* - P_o$. The segments of the lines on

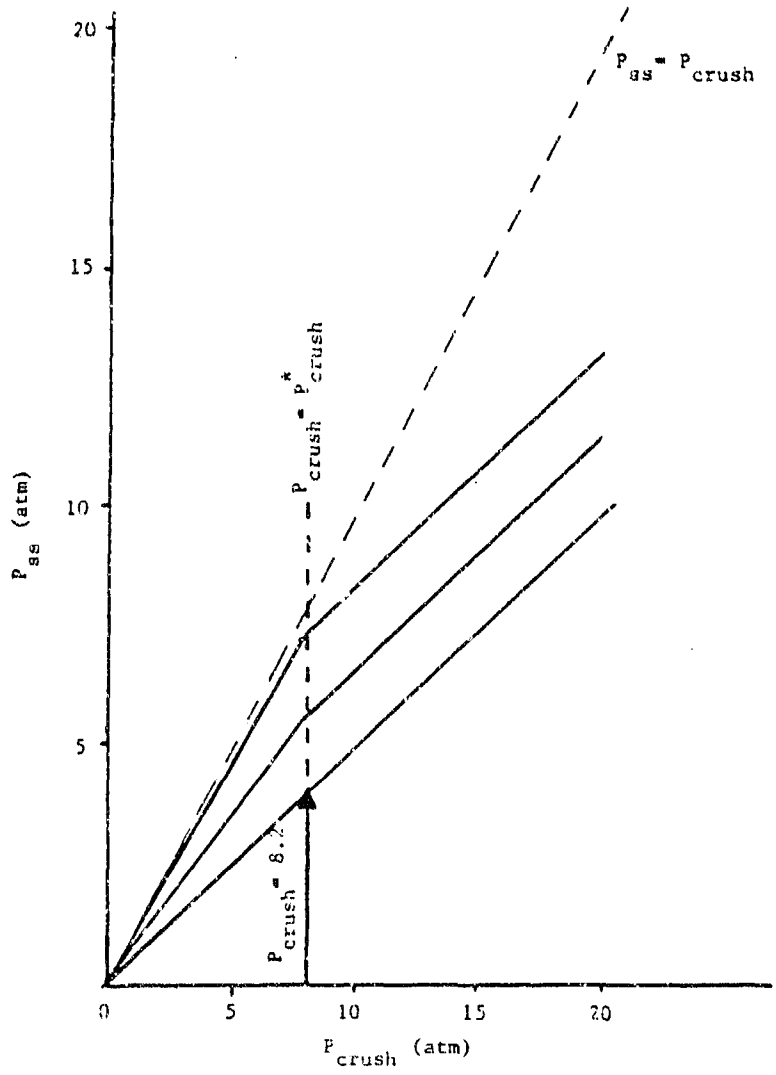

Fig. 4. Variation of P_{ss} versus P_{crush} for various numbers of bubbles. These data are taken from a study of bubble nucleation in gelatine by Yount [11].

either side of this critical point are more or less linear. This behavior is explained as follows. For modest values of P_{crush} the skin remains permeable to gas diffusion. This enables the gas inside the nucleus to remain in equilibrium with the dissolved gas in the gelatin. However, at a critical ambient pressure, $P^{*}=P_{o}+P_{crush}$, the skin molecules become so tightly packed tha che skin becomes essentially impermeable to gas diffusion. This prevents the interior and exterior of the bubble from remaining in equilibrium. Therefore, the gas pressure inside the bubble will be less than the gas pressure of the saturated gelatin, resulting in a lower "effective" P_{ss} during decompression. Throughout decompression the skin is always permeable, independent of P_{crush}. This process gives rise to the name "varying-permeability".

Perhaps it is useful to point out that for acoustic processes $P_{crush}=P_{ss}$ and that the holding time is usually too short for any significant gas diffusion to occur.

D. Crevice model.

The crevice model is fundamentally different from the other models discussed. Its stabilization mechanism does not require that surface tension be nullified, rather, it uses surface tension, combined with geometrical considerations. to stabilize a gas pocket at the bottom of a crevice. It is, perhaps, the most familiar of the models. This is partly true because it can account for a wide range of experimental data, whereas the other models can account for only limited sets of data, most often that of the model's proponent. Since the crevice model has undergone several revisions, it would be unreasonable to discuss all of them in detail. Therefore, the model will be discussed briefly in the form reported by Atchley [16].

The crevice model assumes that gas pockets are stabilized at the bottom of conical cracks or crevices found on hydrophobic solid impurities present in the water. The essential features of the model are depicted in figure 5. When the liquid is saturated with gas, the liquid-gas interface is essentially flat. However, when the liquid is degassed, the interface bows toward the apex of the crevice. This behavior occurs for the following reason. In a saturated solution, the dissolved gas pressure, P_g, equals the pressure which the liquid exerts on the interface. We call this the liquid pressure, P_L, and define it to be the sum of all the pressures present--hydrostatic and acoustic. Diffusion maintains the gas pressure in the nucleus at the dissolved gas pressure. Assuming that vapor pressure is negligible for the time being, we have $P_L=P_g$ for saturated solutions. Since there is no pressure difference across the interface, it is flat and the Laplace pressure ($2\sigma/r$, where σ = surface tension and r = radius of curvature of the interface) is zero. When the liquid is degassed, P_g is less than P_L and the interface bows toward the apex. This curvature give rise to a Laplace pressure which exactly equals the difference between P_L and P_g. Since all pressures are now balanced, the nucleus does not dissolve and remains intact.

Suppose we have a degassed liquid and the liquid pressure is increased. In response to this condition, the interface bows inward more, until it reaches the advancing contact angle. At this point any subsequent motion of the interface involves the entire interface advancing as a whole toward the apex. As it advances, the radius of curvature necessarily becomes smaller, since the angle of the interface measured from the crevice wall is now fixed. As the radius of curvature decreases, the Laplace pressure increases, eventually becoming high enough to balance the increased liquid pressure.

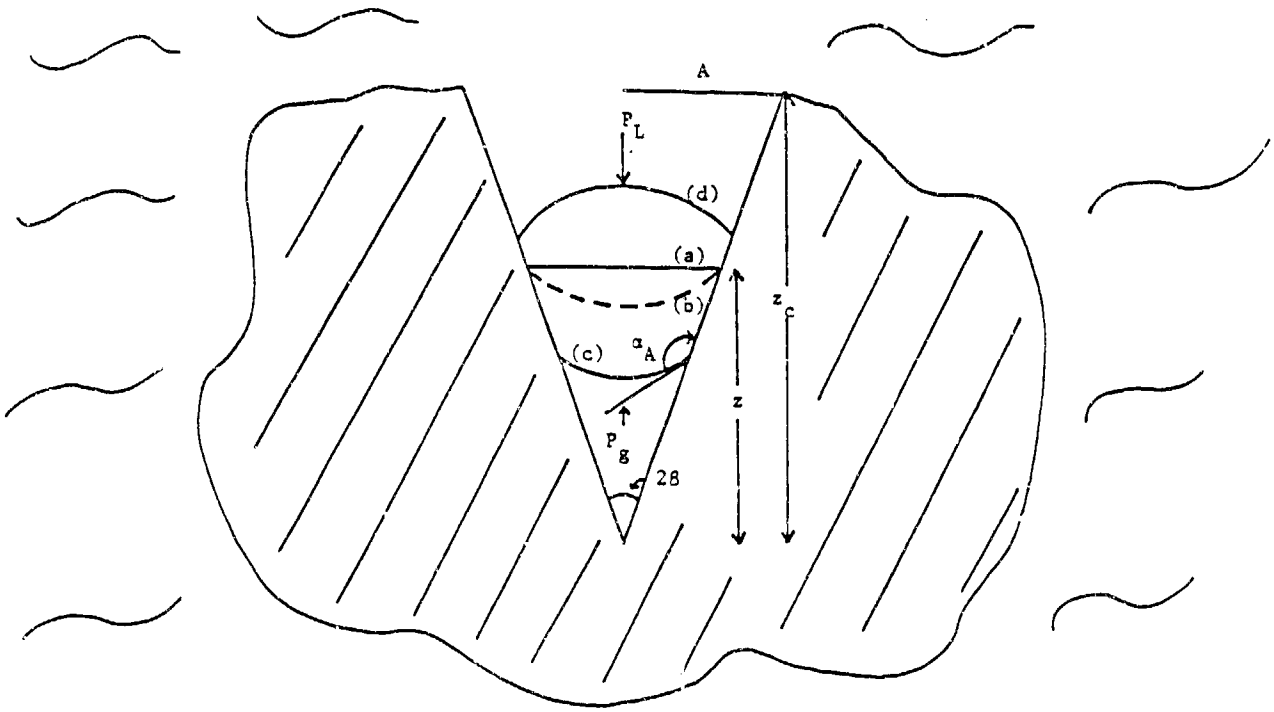

Fig. 5. Diagram of a crevice model that depicts the motion of the interface during the various phases of the nucleation process.

If the liquid pressure is now suddenly decreased to become negative, as during that portion of an acoustic cycle, the interface bows outward and may reach the receding contact angle. If the receding contact angle is reached, any subsequent motion of the interface involves the entire interface receding away from the apex. This recession results in a decrease in the Laplace pressure, since the radius of curvature increases. With the Laplace pressure decreased the gas pressure inside the nucleus is retarded even less. It has been previously assumed [17-20] that the criterion for nucleation from a crevice was that the interface must reach the receding contact angle. It was argued that once the interface had reached the receding contact angle, any subsequent interfacial motion would increase the radius of curvature, resulting in less Laplace pressure (which was now opposing the growth of the nucleus) and so the growth would be unbounded. It was shown by Atchley and Prosperetti [21] that this criterion needs to be modified in the following manner. Reaching the receding contact angle is only a necessary condition for nucleation. It may not however, be sufficient. The receding interface may not grow without bound unless the interface has reached the "critical radius". We consider now the meaning of this term.

The concept of a critical radius was probably first discussed by Harvey [17] though not in a quantitative manner; Blake [22], however, first applied it to cavitation inception while Prosperetti [23] first examined it for the case of a vapor-filled cavity. A derivation is now given for the critical radius of a gas-filled cavity; the corresponding equation for the vapor case will also be obtained.

i. gas-filled cavity

Consider a gas filled bubble of radius R surrounded by a liquid which

exerts a pressure P_L on the bubble. The liquid-gas surface tension is τ. The gas pressure inside the bubble is P_g; the vapor pressure, P_v, is assumed negligible. Assume the bubble is in equilibrium so that the pressure inside, P_g, equals the liquid pressure plus the Laplace pressure due to the surface tension, i.e.

$$P_g = P_L + 2\sigma/R. \tag{1}$$

Simultaneously, the system must be in diffusion equilibrium. This requires

$$c_L = a\, c_i\ , \tag{2}$$

where c_L and c_i refer to the concentrations of gas dissolved in the liquid and present inside the bubble, respectively; a is the solubility coefficient of the gas in the liquid. If the gas is ideal then (2) becomes

$$P_g = BTC_L/a, \tag{3}$$

where B is the universal gas constant and T is the absolute temperature. Equation (3) is a form of Henry's Law. At equilibrium P_g may be replaced with τ, called the gas tension, which is a measure of the partial pressure of the gas dissolved in the liquid. At equilibrium

$$P_g = P_L + 2\sigma/R = \tau \tag{4}$$

or

$$\tau - P_L = 2\sigma/R. \tag{5}$$

The critical (equilibrium) radius is, therefore,

$$R_{cg} = 2\sigma/(P_g - P_L). \tag{6}$$

The subscript "cg" refers to the critical radius for a bubble to grow by gaseous diffusion. Notice that the radius of curvature is positive only in

supersaturated solutions. Since a negative radius is meaningless for free bubbles, stability can occur only in supersaturated solutions.

ii. (mostly) vapor-filled cavity

This discussion is similar to the previous one, except now the efffect of vapor pressure is included. Again, at equilibrium the following condition holds

$$P_v + P_g = P_L + 2\sigma/R. \tag{7}$$

The condition given by equation (3) is dropped and the amount of gas inside the bubble is fixed. In other words, no diffusion of gas takes place. However, the amount of vapor is not fixed. If the gas is ideal then rearranging (7) gives

$$P_L + 2\sigma/R = 3nBT/(4\pi R^3) + P_v \tag{8}$$

where n is the number of moles of the gas inside the bubble. To examine its stability consider the effect of a small increase in R. For the bubble not to grow spontaneously, the effective external pressure, which is given by the left-hand side of equation (8), must increase more than the internal pressure, given by the right-hand side of equation (8). This will always be true if $P_L \geq P_v$, because the gas pressure decreases more with an increase in R than does the Laplace pressure. If, however, $P_L < P_v$ then the situation is different.

The stability criterion can be expressed, in general, as

$$\frac{\partial}{\partial R}\,(P_L + 2\sigma/R) \;>\; \frac{\partial}{\partial R}\,(3nBT/(4\pi R^3) + P_v). \tag{9}$$

Performing the differentiation and solving for R gives

$$R < 4\sigma/[3(P_v - P_L)]. \tag{10}$$

In other words, when $P_v > P_L$, the bubble will be stable against spontaneous

growth only if $R < R_{cv}$ where

$$R_{cv} = 4\sigma/[3(P_v - P_L)] \quad . \tag{11}$$

That is to say, a bubble will grow in a spontaneous unbounded manner when the liquid pressure is less than the vapor pressure only if $R \geq R_{cv}$. A bubble that grows in this way will be mostly vapor-filled. Therefore, the subscript "cv" refers to the critical radius for a vapor bubble to grow from a gas-filled nucleus. The reader is referred to Propseretti [23] for more details.

In the preceding section, the conditions for the nucleation of both gaseous and vaporous bubbles were developed. Using them, expressions will now be given for the applied pressures required for nucleation from gas-filled crevices. These are referred to as cavitation thresholds. It should be noted that the applied pressure, P_A, is equal to the liquid pressure minus the ambient static pressure; i.e., $P_A = P_L - P_o$. (P_A experimentally is the applied acoustic pressure amplitude.) The expressions given below will be for two distinct cases: one for $P_L < P_v$ and the other for $P_L \geq P_v$. This division is a natural one; the difference in the restrictions on P_L is in a sense the difference between acoustic cavitation and diffusion cavitation. Acoustic cavitation is produced by negative applied pressures and its nucleation usually involves the growth of vapor-filled bubbles, although not always. On the other hand, diffusion cavitation is usually produced by ambient pressures greater than the vapor pressure and gas diffusion is the predominant mechanism in its nucleation. Diffusion cavitation should not be confused with gaseous (stable) acoustic cavitation; the two occur in different regions of ambient pressures. Acoustic cavitation is considered first.

Assume that a deep crevice, partially filled with gas, exists in a

hydrophobic solid surrounded by a gas-saturated liquid. The hydrostatic pressure due to the liquid is negligible and the crevice is exposed to an ambient pressure P_o (refer to figure 5). The liquid-gas interface contacts the crevice wall at a height z above the apex. The crevice angle is 2β. The system is in equilibrium, so

$$P_o = \tau = P_g. \tag{12}$$

For temperatures far below the boiling point, $P_v << P_o$ and thus the interface is essentially flat.

The liquid is now degassed so that $\tau < P_o$. Gas will diffuse out of the nucleus causing the interface to bow inward, toward the apex, as shown by the dashed line (b) in figure 5. At equilibrium $P_g = \tau$ and

$$P_o = P_g + P_v + 2\sigma/R. \tag{13}$$

The new equilibrium position of the nucleus is shown by the solid line (c) in figure 5. At this position the angle between the interface and the wall is α_A, the advancing contact angle.

At this point, an acoustic field of pressure amplitude P_A is applied such that the liquid pressure exerted on the interface is $P_o + P_A$. Assume P_A is such that $P_v > P_o - P_A$. During the negative half-cycle the interface bows outward and a new equilibrium position is established. A bubble will be nucleated from this new position only if the radius of curvature of the interface is larger than the critical radius R_{cv}. The value of P_A necessary for this condition to be met is found after several pages of algebra by Atchley [16] to be

$$P_A = P_o - P_v + \frac{2}{3^{3/2}} P_g \left[\left(\frac{P_o - P_v}{P_g} - 1\right)^3 \left|\frac{\cos(\alpha_R - \beta)}{\cos(\alpha_A - \beta)}\right|^3 \left(\frac{\cot\beta + \eta_R}{\cot\beta - \eta_A}\right)\right]^{1/2}, \tag{14}$$

where η_i (i=R,A for receding and advancing) is given by

$$n_i = \left[\frac{1}{\delta_i} - \sqrt{\frac{1}{\delta_i^2} - 1} \right] \left[\frac{2}{\delta_i} + \sqrt{\frac{1}{\delta_i^2} - 1} \right], \qquad (15)$$

and $\delta_i = |\cos(\alpha_i - \beta)|$. The n_i's are geometrical terms associated with the crevice.

As shown by Atchley [16], this equation accurately predicts the measured dependence of the acoustic cavitation threshold of water with (a) dissolved gas content, (b) liquid surface tension and (c) liquid temperature. Shown in Figs. 6 and 7 are the comparisons between this theory and previously published experimental measurements for cases (a) and (b).

In Fig. 6 the predicted variation of the cavitation threshold with dissolved gas content is compared with three different sets of experimental measurements. One can see that the theory gives a reasonably good representation of the data. Two important points are to be noted. First, the line labelled P_A^* is the theoretical prediction based on the assumption that a cavity is nucleated when the interface reaches the receding contact angle; the line labelled P_A is for the condition that the interface reaches the critical radius. It is seen that the receding contact angle criterion predicts a finite threshold at zero gas pressure, an unreasonable result. This failure of the theory is corrected in the critical-radius version. Second, the data of Galloway [24] indicate that as more and more gas is removed, the threshold rises very rapidly and apparently does not approach a finite value, a result consistent with the critical-radius version of the crevice model theory. A caveat is offered: the data of Galloway have always been suspect because they have such large absolute numbers.

In Fig. 7 the predicted variation of the cavitation threshold with surface tension is compared with the experimental measurements of Crum [19] for two values of the dissolved gas concentration. Again one sees an excellent agreement between measured and predicted values. It should be

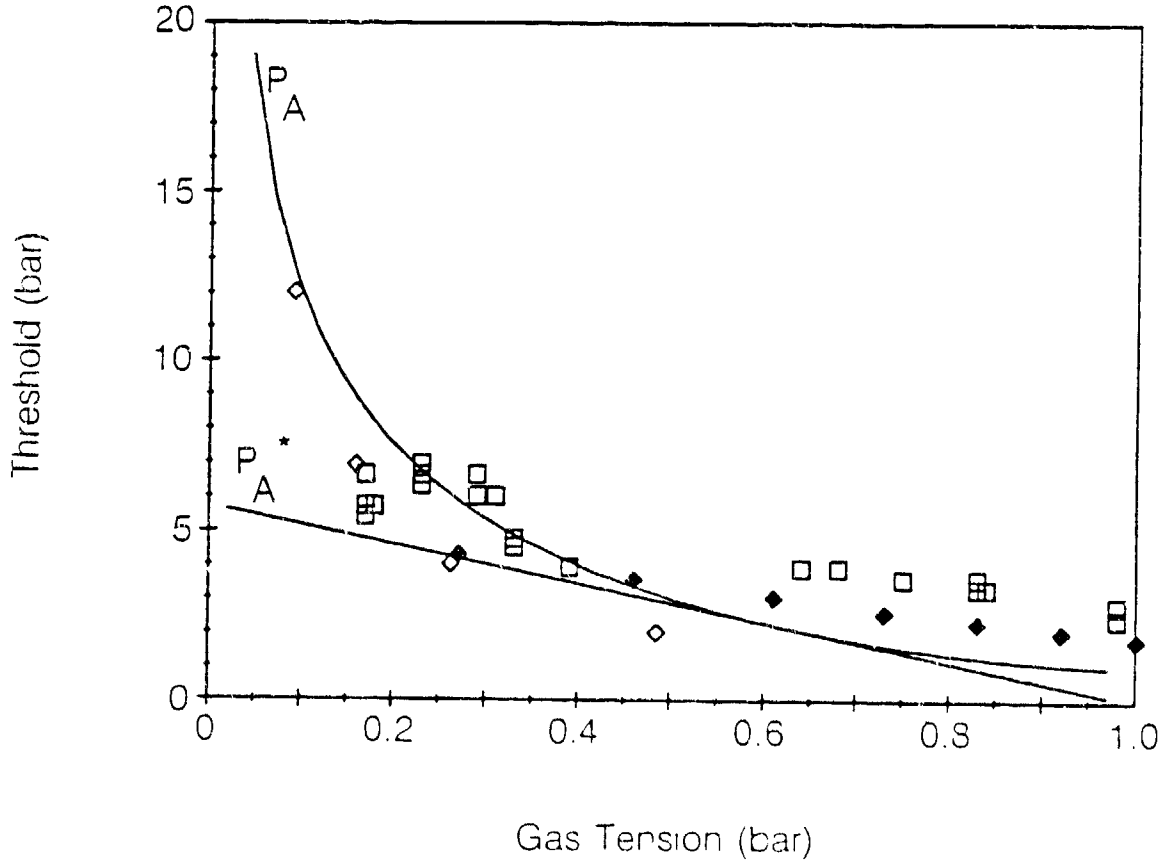

Fig. 6. Variation of the acoustic cavitation threshold with dissolved gas concentration for water. The various symbols indicate the results of Strasberg (□), Galloway (◇) and Connolly and Fox (◆). The line labelled P_A requires the critical radius be achieved before nucleation can occur; The line labelled P_A^* requires only that the receding contact angle be reached.

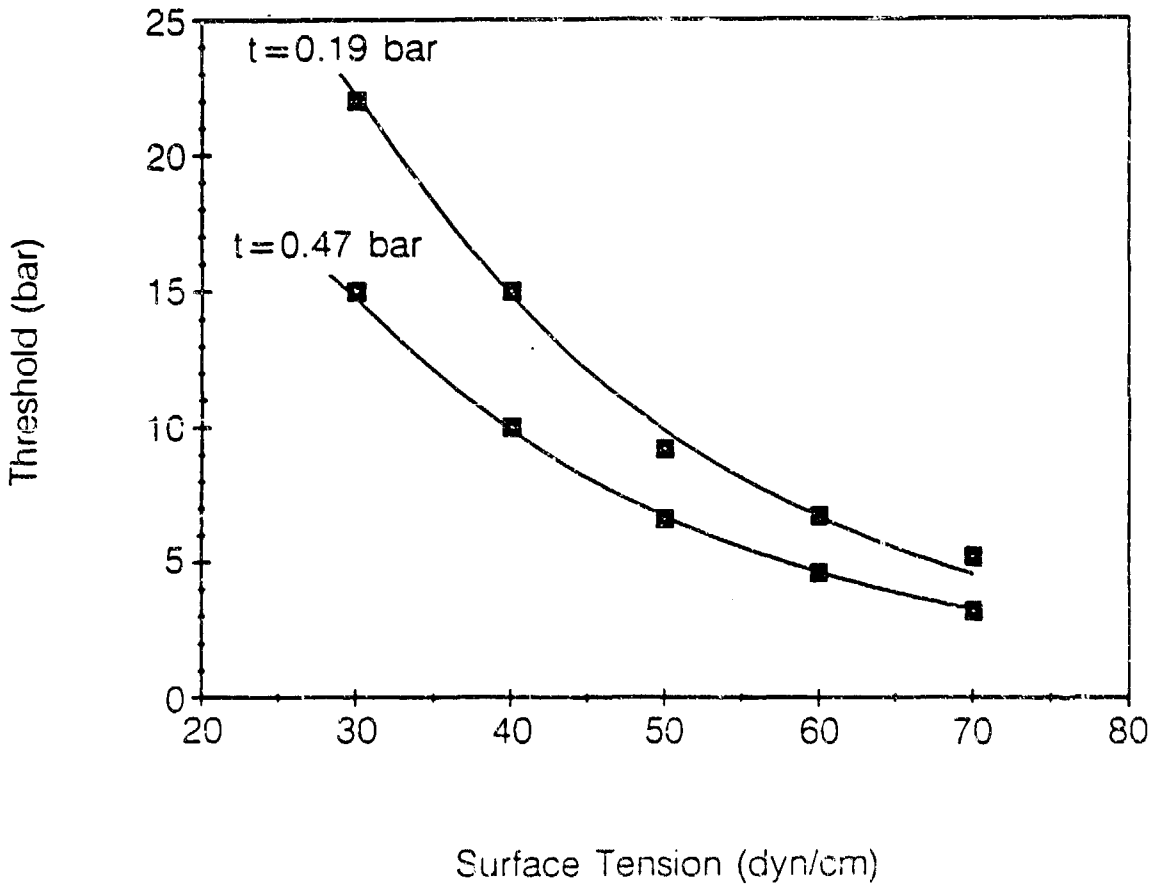

Fig. 7. Variation of the acoustic cavitation threshold of water with surface tension. The symbols are the data of Crum and the solid lines are calculated from equation (14) using $\beta = 12.85^{\circ}$ and $\alpha_H = 22.15^{\circ}$ for $P_g = 0.47$ and $\beta = 10.8^{\circ}$ and $\alpha_H = 24.2^{\circ}$ for $P_g = 0.19$ bar.

noted that there is some "fitting" here in that in the theory there are three unknown constants: the equilibrium contact angle α_E (which is set equal to the advancing contact angle α_A), the hysteresis angle α_H (which is the difference between the advancing and receding contact angles), and the crevice angle (2β). In Atchley's analysis, the equilibrium contact angle is set to a value appropriate for water on nonpolar solids such as paraffin and beeswax, the hysteresis angle and crevice angle may be varied with the constraints that the hysteresis angle lie within the published angle of values for water on nonpolar solids (14^o-- 35^o) and the crevice angle be small (less than 15^o).

Finally, comparison of the predicted and measured variation of the cavitation threshold with temperature also show excellent agreement, when the temperature dependence of the surface tension, dissolved gas pressure and vapor pressure are introduced into the theory. For brevity, these results are not included in this report.

In summary, it is seen that the critical-radius version of the crevice model can acurately explain the measured variations of the cavitation threshold of water with most of its physical parameters. (The anomaly with the dissolved ion concentration being one exception.) Accordingly, it is reasonable to assume that the most acceptable model for cavitation nuclei in water at this time is the crevice model.

E. Nucleation in tissue

It seems in order at this point to move from experiments in the relativly simple medium of water and consider the implications of cavitation nucleation in biological systems. At this stage of research, very little can be said conclusively in a scientific sense. However, there are several observations that will now be tabulated that address this issue.

1. Nuclei exist in tissue and can be activated acoustically.

A large number of experiments have been performed to determine the nature of *in vivo* cavitation nuclei and probably the most that can be said is that all of these experiments indicate that these nuclei do indeed exist. To single out a few of the many experiments [25-32] that demonstrate this fact, let me call attention to four important ones:

Ter Haar et.al. [25-26] have irradiated live guinea pig legs with therapeutic ultrasound while examining the irradiated area with a diagnostic scanner. They observed the development of echo centers that were attributed to gas bubbles (the echos went away when a static pressure was applied) within the tissue. Several sites developed within the radiated areas at modest acoustic intensities. There is good reason to believe that these bubbles of microscopic size (greater than 20 μm in diameter) grow from preexisting nuclei within the guinea pig by a process called rectified diffusion [27], a phenomenon which shall be described later in this article.

Carstensen et.al. [28-29] have irradiated Drosophilla eggs and larvae at various stages in their development with pulsed ultrasound. They have determined that when gas-containing trachea developed in the organisms, they were extremely suceptable to the ultrasound and large fractions could be killed.

Hemmingsen et.al. [30-31] have observed bubble formation in crustaceans following decompression from hyperbaric gas exposures. Photographs are presented showing the presence of these bubbles within these living organisms.

Frizzell et.al. [32] have observed hind limb paralysis in mouse neonates upon irradiation with high intensity CW ultrasound. Furthermore, the effect was surpressed by the application of a static pressure. They

concluded that cavitation was the damage mechanism, which implies that there must have been nuclei present within the neonate before radiation.

2. The stabilization mechanism is unknown.

Because the cavitation nucleus is so small compared to the microscopically visible bubble that is eventually observed, there is essentially no memory of the initial state. Thus, although it is widely believed that visible cavitation bubbles arise from stabilized nuclei, there is little evidence concerning the actual stabilization mechanism. Some observations from the literature may be helpful, however. Although it doesn't seem unreasonable that biological fluids could contain small microscopic solids on the order of a few microns in size (crevices that can stabilize gas pockets are probably on the order of tenths of microns), the multiple set of filters (e.g. lungs, liver) that the body possesses that would tend to remove these objects makes this stabilization model appear less likely than others. However, Fraser et.al. [33] have examined bubbles produced in the inner ears of squirrel monkeys and have found indications that the origins of these bubbles are sharp crevices in the bony tissues. Microscopic studies of the damage sites tend to lend support to this view. Several earlier studies [34-35] have examined the details of the nucleation process.

At first thought, the variety of salts present in most biological fluids would support a stabilization model similar to that proposed by Aculichev [6], in which microscopic gas bubbles are surrounded with hydrophobic ions that prevent bubble dissolution by Coulomb repulsion. There appears to be a serious problem with the origin of the nuclei however. In Aculichev's model, the ions are presumed to migrate to the surface of preexisting dissolving gas bubbles and eventually prevent these bubbles from further dissolution. However, there doesn't appear to be a mechanism

for introducing the initial pocket of gas into the biological system without first having it stabilized.

This chicken-and-the-egg problem is faced in a similiar fashion with Yount's [11-15] surface-active agent model. Again there is a requirement that preexisting dissolving gas bubbles are stabilized by the organic skin. Yount does have evidence that very small [< 0.1 μm] apparently stabilized spherical gas bubbles are present in water; whether these objects could pass directly into the blood stream for distribution throughout the body is still in question.

A solution to the "seeding" problem of nuclei within biological systems is avoided by a model for nucleation favored by Hemmingsen [30, 36]. He suggests that the relative movement of one tissue over the other developes sufficient negative pressures to introduce pockets of free gas by a technique known as tribonucleation. The process is fairly well known and has been suggested earlier as a nucleation mechanism. The strength of Hemmingsen's case is made on the basis of his studies of decompression in various tranparent crustaceans. When the limbs of these animals are restricted from movement, the decompression pressures required to induce bubble formation is greatly raised. When the limbs are free to move, however, bubble formation occurs at much lower decompression pressures. Furthermore, the observable bubbles tend to be concentrated near the joints where considerable relative tissue movement occurs. The fact that bubble formation in divers occurs more frequently and at an earlier stage in elbows and knees tends to lend corroborating evidence to this suggestion [37]. Furthermore, exercise immediately after decompression increases the incidence of symptoms in divers [38] and decreases the altitude threshold for aviators [39]. Showers of bubbles have been detected in the circulatory system of divers immediately after arm movements [40].

On the other hand, the phenomenon of tribonucleation is still not well-defined [31] and has not yet been applied successfully to experimental data as the crevice model [16] and the organic skin model [15].

3. The acoustic activation can be potentially damaging.

Whenever a pocket of gas is caused to pulsate by the action of a relatively intense acoustic field, it has three possible behaviors: (i) it can remain unchanged in time-average volume, but pulsate violently, (ii) it can grow explosively in one or two cycles (transient cavitaiton), or (iii) it can grow slowly by rectified diffusion to a point where (a) it breaks up due to surface wave formation, or (b) it grows explosively as in (ii).

For all of these cases, if the spatial peak temporal peak acoustic pressure amplitude is above a value of a few atmospheres, there is a significant potential for damage to biological tissue. The damage may occur due to three different mechanisms associated with this violent pulsation: (1) When a bubble pulsates violently for several cycles it causes severe shear streses in the vicinity of the bubble, which can cause significant biological effects [41-45]; (2) when a bubble grows explosively and collapses, it can develop shock waves and imploding jets that have caused severe damage to surrounding boundaries [46-48]; (3) if the bubble grows by rectified diffusion to radii that are submultiples of its resonance size, it can pulsate violently enough to cause sonoluminescence. This light emission is probably an indication of the production of highly reactive free radicals [49-52] that are the same damage mechanism as ionizing radiation.

We can conclude this section with the following observations:

A. Microscopic pockets of gas can be stabilized against dissolution by a variety of physical mechanisms.

B. These gas pockets can be activated acoustically.

C. The acoustically activated bubbles can have harmful bioeffects.

II. Rectified Diffusion

A. Introduction

A concept that can be of general interest in the area of ultrasonic bioeffects is the mechanism wisely labelled as "rectified diffusion". This process involves the relatively slow growth of a pulsating gas bubble due to an average flow of mass (gas) into the bubble over an acoustic cycle. This "rectification of mass" is a direct consequence of the applied sound field and can be of importance wherever the applied acoustic pressure amplitude exceeds the threshold for rectified diffusion (on the order of a few tenths of an atmosphere for typical values of the acoustic frequency and bubble radius.) For liquids that are not supersaturated with gas, a definable threshold exists due to the Laplace pressure exerted on the gas contained within a bubble by the force of surface tension. The value of this pressure is given by $P_i = 2\sigma/R_n$, where P_i is the internal pressure, σ is the surface tension of the liquid, and R_n is the equilibrium radius of the bubble.

For relatively large gas bubbles, on the order of 1 cm in diameter, say, this pressure is quite small (<0.001 bar). However, for bubbles on the order of 1 μm in diameter, this pressure can be quite significant (>1.0 bar). Thus, when one considers the stability of a free gas bubble in a liquid with a surface tension similar to that for water, they must be stabilized in some manner as described earlier, or they will dissolve rapidly.

With the application of an applied sound field, however, a bubble can be made to oscillate about an equilibrium radius and caused to grow in size because of the following effects.

The first effect is an "area" effect. When the bubble contracts, the concentration of gas (moles $-l^{-1}$) in the interior of the bubble increases,

and gas diffuses from the bubble. Similarly, when the bubble expands, the concentration of gas decreases, and gas diffuses into the bubble. Since the diffusion rate is proportional to the area, more gas will enter during expansion than will leave during the contraction of the bubble; therefore, over a complete cycle, there will be a net increase in the amount of gas in the bubble.

The second effect is the "shell" effect. The diffusion rate of gas in a liquid is proportional to the gradient of the concentration of dissolved gas. Consider a spherical shell of liquid surrounding the bubble. When the bubble contracts, this shell expands, and the concentration of gas near the bubble wall is reduced. Thus, the rate of diffusion of gas away from the bubble is greater than when the bubble is at its equilibrium radius. Conversely, when the bubble expands, the shell contracts, the concentration of gas near the bubble is increased, and the rate of gas diffusion toward the bubble is greater than average. The net effect of this convection is to enhance the rectified diffusion. It has been shown that both the area and the shell effects are necessary for an adequate description of the phenomenon.

Apparently, rectified diffusion was first recognized by Harvey [17], who considered the biological implications of the effect as early as 1944. Blake [22] was probably the first to attempt a theoretical explanation and his predictions were nearly an order of magnitude too small, because he considered only the area effect. An adequate theory was first presented by Hsieh and Plesset [53] who were the first to include the effect of convection. Strasberg [54], who had made some experimental measurements, showed that the theory of Hsieh and Plesset [53] generally agreed with his measurements. Eller and Flynn [55] extended the analysis to include

nonlinear or large amplitude effects by treating the boundary condition of the moving wall in a slightly different way. Safar [56] showed that the Hsieh-Plesset results were essentially equivalent to those of Eller and Flynn [55] when inertial effects were added to the Hsieh-Plesset approach.

The few measurements obtained by Strasberg were extended by Eller [57] to include both the threshold and the growth rate. He found that the theory was adequate in predicting the thresholds for growth by rectified diffusion but was unable to account for some large growth rates that he observed. He suggested that acoustic streaming may be the cause of the larger-than-predicted rates of growth. Gould [58] was able to directly observe gas bubble growth by rectified diffusion through a microscope and discovered that growth rates could be greatly enhanced by the onset of surface oscillations of the bubble, which in turn seemed to induce significant acoustic microstreaming. Attempts by Gould [58] to apply the acoustic streaming theories of Davidson [59] and of Kapustina and Statnikov [60] to explain his results were not successful. Extended theoretical treatments were presented by Skinner [61] and Eller [62] to account for growth through resonance.

Additional measurement of the growth of gas bubbles by rectified diffusion were later obtained by Crum [63] who made both threshold and growth rate measurements for a variety of conditions. He extended the theory to include effects associated with the thermodynamic behavior of the bubble interior and found excellent agreement between theory and experiment for both the rectified diffusion threshold and the growth rate for air bubbles in pure water. Anomalous results were obtained, however, when a small amount of surfactant was added to the water. The rate of growth of bubbles by rectified diffusion increased by a factor of about five when the surface tension was lowered by a factor of about two, with no

discernible surface wave activity. Although some increase is predicted, the observed growth rates were much higher. A slight reduction in the threshold with reduced surface tension was also observed. Some explanations offered by Crum [63] for this anomalous behavior were that there was some rectification of mass due to the surfactant on the surface of the bubble and/or there was microstreaming occurring even in the absence of surface oscillations.

To bring our limited review of the literature up to date, it is noted that there have been recent applications of the equations of rectified diffusion to studies of the threshold for growth of microbubbles in biological media [43], the threshold for cavitation inception [64], and as a possible explanation for the appearance of gas bubbles in insonified guinea pigs [65]. Finally, a comprehensive paper on rectified diffusion was recently published by Crum [66] and can be referred to for details.

B. The Governing Equations

A brief outline of the theory is now given, complete with the detailed equations to be used to make calculations of the threshold and the growth rate of bubbles by rectified diffusion. A complete mathematical description of the growth of a gas bubble by rectified diffusion would require an equation of motion for the bubble, diffusion equations for the liquid and the interior of the bubble, and heat conduction equations for both the liquid and the bubble. Continuity relations at the bubble wall would be required, and the situation is further complicated by the fact that these equations are coupled. Since this general approach presents a very formidable mathematical problem, various simplifications are required to obtain a solution.

The approach used by Hsieh and Plesset [53] and by Eller and Flynn

[55] is to separate the general problem into an equation for the motion of the bubble wall, and a diffusion equation for the concentration of gas dissolved in the liquid alone. We will use as the equation of motion for the gas bubble the well-known Rayleigh-Plesset [67] equation, given here by

$$R\ddot{R} + \frac{3}{2}\dot{R}^2 + \frac{1}{\rho}\{P_o[1-(R_o/R)^{3\eta}] - P_A \cos \omega t + \rho R_o \omega_o b\dot{R}\} = 0, \tag{16}$$

where R and R_o are the instantaneous and equilibrium values of the bubble radius respectively, ρ is the liquid density, η the polytropic exponent of the gas contained within the bubble, P_A the acoustic pressure amplitude, ω the angular frequency, ω_o the small-amplitude resonance frequency and b is a damping term applied to the bubble pulsations. It is assumed that the damping is only important near bubble resonance and thus the expressions for the specific damping terms are only applicable near resonance.

Further, $P_o = P_\infty + 2\sigma/R_o$ where P_∞ is the ambient pressure and σ is the surface tension of the liquid. The small amplitude (linear) resonance frequency of the bubble, ω_o, is given by

$$\omega_o^2 = (1/\rho R_o^2)(3\eta P_o - 2\sigma/R_o). \tag{17}$$

The diffusion equation for the gas in the liquid is Fick's law of mass transfer and is given by

$$dc/dt = \partial C/\partial t + \underset{\sim}{v}\cdot \nabla C = D\nabla^2 C, \tag{18}$$

where C is the concentration of gas in the liquid, $\underset{\sim}{v}$ is the velocity of the liquid at a point, and D is the diffusion constant. The coupling between (16) and (18) is through the convective term $\underset{\sim}{v}\cdot\nabla C$, and represents a major difficulty in the solution. This term was neglected by Blake [22] and

resulted in a prediction for the threshold that was an order of magnitude too small. The problem with the moving boundary has been solved in two slightly different ways by Hsieh and Plesset [53] and by Eller and Flynn [55]. The details of their solutions can be found in their respective works; the solution of the latter will be used here.

It is shown by Eller and Flynn [55] that the time rate of change in the number of moles n of gas in a bubble is given by

$$dn/dt = 4\pi D R_o C_o \times \left[\langle R/R_o \rangle + R_o \left(\frac{\langle (R/R_o)^4 \rangle}{\pi D t} \right)^{1/2} \right] H, \tag{19}$$

where C_o is the 'equilibrium' or 'saturation' concentration of the gas in the liquid in moles (unit volume)$^{-1}$, the pointed brackets imply time average, t is the time, and H is defined by

$$H = C_i/C_o - \langle (R/R_o)^4 \, (P_g/P_\infty) \rangle / \langle (R/R_o)^4 \rangle. \tag{20}$$

Here C_i is the concentration of dissolved gas in the liquid far from the bubble and P_g, the instantaneous pressure of the gas in the bubble, is given by

$$P_g = P_o (R_o/R)^{3n}. \tag{21}$$

As seen by the above equation, a polytropic exponent assumption is made for the pressure of the gas in the interior of the bubble. This assumption is commonly made and is probably reasonably accurate for small-amplitude pulsations. There is evidence that it needs to be modified for moderate to large amplitude oscillations, however.

The values of R/R_o to be used in the equations above are obtained

by an expansion solution of (16) in the form

$$R/R_o = 1 + \alpha(P_A/P_\infty)\cos(\omega t + \delta) \qquad (22)$$

$$+ \alpha^2 K(P_A/P_\infty)^2 + \ldots$$

where it has been determined that

$$\alpha^{-1} = (\rho R_o^2/P_\infty)[(\omega^2 - \omega_o^2)^2 + (\omega\omega_o b)^2]^{1/2}, \qquad (23)$$

$$K = \frac{(3\eta + 1 - \beta^2)/4 + (\sigma/4R_0P_\infty)(6\eta + 2 - 4/3\eta)}{1 + (2\sigma/R_oP_\infty)(1 - 1/3\eta)}, \qquad (24)$$

$$\delta = \tan^{-1}[\omega\omega_o b/(\omega^2 - \omega_o^2)], \qquad (25)$$

and

$$\beta^2 = \rho\omega^2 R_o^2/3\eta P_\infty . \qquad (26)$$

It is necessary to know the damping of the bubble pulsations when the bubble is driven near resonance. This damping has been calculated by Eller [68] using the expressions of Devin [69]; a similar but not identical value for the damping term has also been obtained by Prosperetti [67].

Because the pressure in the interior of the bubble is assumed to be given through the polytropic exponent approach, an accurate expression for the thermal damping can not be given. Prosperetti [67] has shown that an estimate of this damping can be expressed through an "effective viscosity". Since the damping is only important near resonance (or at harmonics and subharmonics of the resonance frequency), and since the rectified diffusion equations are probably not accurate near resonance anyway, this nonrigorous approach will be followed for the present time.

The total damping constant, b, is assumed to be able to be written as a sum of contributions due to the three common damping mechanisms, viz., thermal, viscous and radiation:

$$b = b_t + b_v + b_r,$$

where

$$b_t = 3(\gamma-1)\left[\frac{X(\sinh X + \sin X) - 2(\cosh X - \cos X)}{X^2(\cosh X - \cos X) + 3(\gamma-1)X(\sinh X - \sin X)}\right] \quad (26)$$

with

$$X = R_o(2\omega/D_l)^{1/2}, \quad (27)$$

and

$$b_v = 4\omega\mu/3\eta P_\infty, \quad (28)$$

$$b_r = \rho R_o^3 \omega^3/3\eta P_\infty\, c, \quad (29)$$

with

$$\eta = \gamma(1 + b_t^2)^{-1}\left[1 + \frac{3(\gamma-1)}{X}\left(\frac{\sinh X - \sin X}{\cosh X - \cos X}\right)\right]^{-1}. \quad (30)$$

In these equations γ is the ratio of specific heats and $D_l = K_l/\rho_l C_{pl}$, where K_l is the thermal conductivity of the gas in the bubble, ρ_l is the density of gas, C_{pl} is the specific heat at constant pressure for the gas, and μ is the viscosity and c is the speed of sound, both in the liquid. To obtain a usable expression for the growth-rate equation, the time averages $\langle R/R_o\rangle$, $\langle(R/R_o)^4\rangle$, and $\langle(R/R_o)^4\,(P_g/P_\infty)\rangle$ are required. It is found that

$$\langle R/R_o\rangle = 1 + K\alpha^2(P_A/P_\infty)^2 \quad (31)$$

$$\langle(R/R_o)^4\rangle = 1 + (3 + 4K)\,\alpha^2\,(P_A/P_\infty)^2 \quad (32)$$

and

$$\langle(R/R_o)^4(P_g/P_\infty)\rangle = \left[1 + \frac{3(\eta-1)\,(3\eta-4)}{4}\,\alpha^2\left(\frac{P_A}{P_\infty}\right)^2 + (4-3\eta)K\alpha^2\left(\frac{P_A}{P_\infty}\right)^2\right]\left[1 + \frac{2\sigma}{R_o P_\infty}\right]. \quad (33)$$

By assuming an ideal gas behavior, we can relate the equilibrium radius to the number of moles of gas by the equation

$$P_o = 3nk\,T/(4\pi R_o^3) \quad (34)$$

where k is the universal gas constant and T is the absolute temperature.

This equation should be a good approximation for small acoustic pressure amplitudes, so that the density fluctuations do not become excessive, and for low host-liquid temperatures, so that the ratio of vapor/gas within the bubble remains low. Such conditions would be met for normal experimental situations.

By combining (19), (20) and (34), an expression is obtained for the rate of change of the equilibrium bubble radius with time:

$$\frac{dR_o}{dt} = \frac{Dd}{R_o}\left[\langle R/R_o\rangle + R_o\left(\frac{\langle (R/R_o)^4\rangle}{\pi Dt}\right)^{1/2}\right]$$

$$\times\left(1+\frac{4\sigma}{3P_\infty R_o}\right)^{-1}\left[\frac{C_i}{C_o} - \frac{(R/R_o)^4(\quad/P_\infty)}{\langle (R/R_o)^4\rangle}\right] \qquad (35)$$

where $d = k\,TC_o/P_\infty$.

In (35), the time averages $\langle R/R_o\rangle$, $\langle (R/R_o)^4\rangle$ and $\langle (R/R_o)^4\,(P_g/P_\infty)\rangle$ are given by (31), (32) and (33), respectively. The threshold acoustic pressure for growth of a gas bubble is obtained by setting $dR_o/dt = 0$, and results in the equation

$$P_A^2 = \frac{(\rho R_o^2\omega_o^2)\,[(1-\omega^2/\omega_o^2)^2 + b^2(\omega^2/\omega_o^2)]\,(1 + 2\sigma/R_oP_\infty - C_i/C_o)}{(3+4K)(C_i/C_o) - \{[3(n-1)(3n-4)/4] + (4-3n)K\}(1 + 2\sigma/R_oP_\infty)} \quad . \qquad (36)$$

These expressions in (35) and (36) are the governing equations for rectified diffusion and enable one to obtain the threshold for inception of growth and the rate of this growth. The growth rate equation (35), also applies below the threshold, and with $P_A = 0$, describes the case for diffusion in the absence of an applied sound field. Although these equations are rather complex, some simple concepts can be obtained by a

cursory examination of their form.

First of all, note in (35) that the rate of growth is directly proportional to the diffusion constant and other physical constants associated with the liquid. Thus, compared with air, helium, which has a higher diffusivity can cause more rapid growth. Also, carbon dioxide, which has a higher solubility in water, can cause more rapid growth.

Note also, in (36) that the minus signs in the numerator of the threshold expression give important indications of gross behavior. For example, the last term in parentheses indicates the reason for a "threshold". Unless the dissolved gas concentration ratio, C_i/C_o, is greater than the non-dimensional surface tension term, $2\sigma/R_o P_\infty$, a positive acoustic pressure amplitude is required. Thus, it is the effect of surface tension that demands that a threshold exists. If C_i/C_c is greater than $2\sigma/R_o P_\infty$, then the system is supersaturated to the point that bubbles will grow spontaneously, without the requirement of an externally-applied acoustic field - as is the case for carbonated beverages. High values of supersaturation probably do not occur within biological tissue, though localized regions within a cell, for example, where respiration may occur and diffusion is restricted may be considerably different from equilibrium conditions within the bulk of a liquid. Ward et.al. [70] have examined such conditions where bubbles are unstable to growth due to localized supersaturation. The caveat here is that the extension of these equations that were developed for simplified conditions within a bulk liquid may not be applied directly to the physiological situation.

A second observation that can be made when examining these equations is that if the bubble is driven near its resonance frequency, the threshold is lowered considerably and is determined essentially by the damping. Since the bubble is a dynamic system, tending to grow toward resonance, a

gas bubble should be expected to undergo very large amplitude pulsations when driven by CW acoustic fields of even moderate intensity.

C. Simplified Equations

The equations for the growth rate, (35) and the threshold, (36), for rectified diffusion are rather complicated mathematical expressions that do not lend themselves very easily to inspection in order to determine the effect of a particular parameter. Further, there are ranges of interest in which the equations can be simplified greatly and still present accurate predictions. Since the threshold for rectified diffusion is normally the desirable quantity, attention will be restricted to that equation alone.

The two principal regions of interest in the study of rectified diffusion are: (i) an area applicable to underwater and physical acoustics where the acoustic frequencies are of the order of a kilohertz and the bubble radii are of the order of tens of μm; (ii) an area applicable to bioacoustics where the frequencies are of the order of a megahertz and the radii on the order of 1 μm.

Since our concern here is primarily with region (ii), the simplified expression for the threshold expresion for this region is now given. In this region, say $\omega = 2\pi(1\ \text{MHz})$ and $R_o = 2\mu\text{m}$, the bubbles will pulsate isothermally, due to their small size, and $\eta \doteq 1.0$. Further, the principal contribution to the damping at this frequency is the viscosity term, so that $b_v >> (b_t,\ b_r)$ and hence $b = b_v$. Finally, for small bubbles, the surface tension term can be quite large and cannot be neglected. With these restrictions, the rectified diffusion threshold applicable to region (ii) is given by

$$P_A^2 = \frac{(\rho R_o^2 \omega_o^2)^2 [1 - \omega^2/\omega_o^2)^2 + b^2]\ [1 + 2\sigma/R_o P_\infty - C_i/C_o]}{(3 + 4k)(C_i/C_o) - K(1 + 2\sigma/R_o P_\infty)}, \tag{37}$$

where

$$K = \frac{(1 - \beta^2/4) + 5\sigma/(3P_\infty R_o)}{1 + 4\sigma/(3P_\infty R_o)}, \tag{38}$$

$$\beta^2 = \rho\omega^2 R_o^2 / 3P_\infty \tag{39}$$

$$b = 4\omega\mu / 3P_\infty, \tag{40}$$

and

$$\omega_o^2 = (1/\rho R_o^2)\ (3P_\infty + 4\sigma/R_o). \tag{41}$$

D. Experimental Technique for Examining Rectified Diffusion

In this section is presented a brief description of the principal experimental technique used to make measurements of growth of bubbles by rectified diffusion. This technique was first utilized by Strasberg [8], with some modifications by Eller [57] and Gould [58].

The main feature of the technique is the isolation of a single gas bubble in an acoustic stationary wave, with the ability to determine the bubble radius accurately and quickly. The specific description of the technique used by Crum [63] is now given. Refer to Fig. 8 for a diagram of the experimental apparatus.

The stationary wave system was constructed by cementing a hollow glass cylinder between two matched hollow cylindrical transducers, fitted with a flexible pressure release diaphragm on one end and open at the other. The composite system was approximately 7.5 cm in diameter by 10 cm in height, with the width of the glass in the middle about 2.5 cm. This system was driven at its (r, θ, z) = (2, 0, 2) mode at a frequency of 22.1 kHz.

When a standing wave exists in the liquid, an acoustic radiation pressure force, commonly called the primary Bjerknes force [71] is exerted on air bubbles that draws them toward a pressure antinode if they are less than resonance size and forces them toward the nodes if they are larger than resonance size. Because of gravity, there is also a constant (essentially) force of buoyancy on a gas bubble in a liquid, and this force is always directed upward. Since the primary Bjerknes force [72] is proportional to the acoustic pressure, which varies with position, there

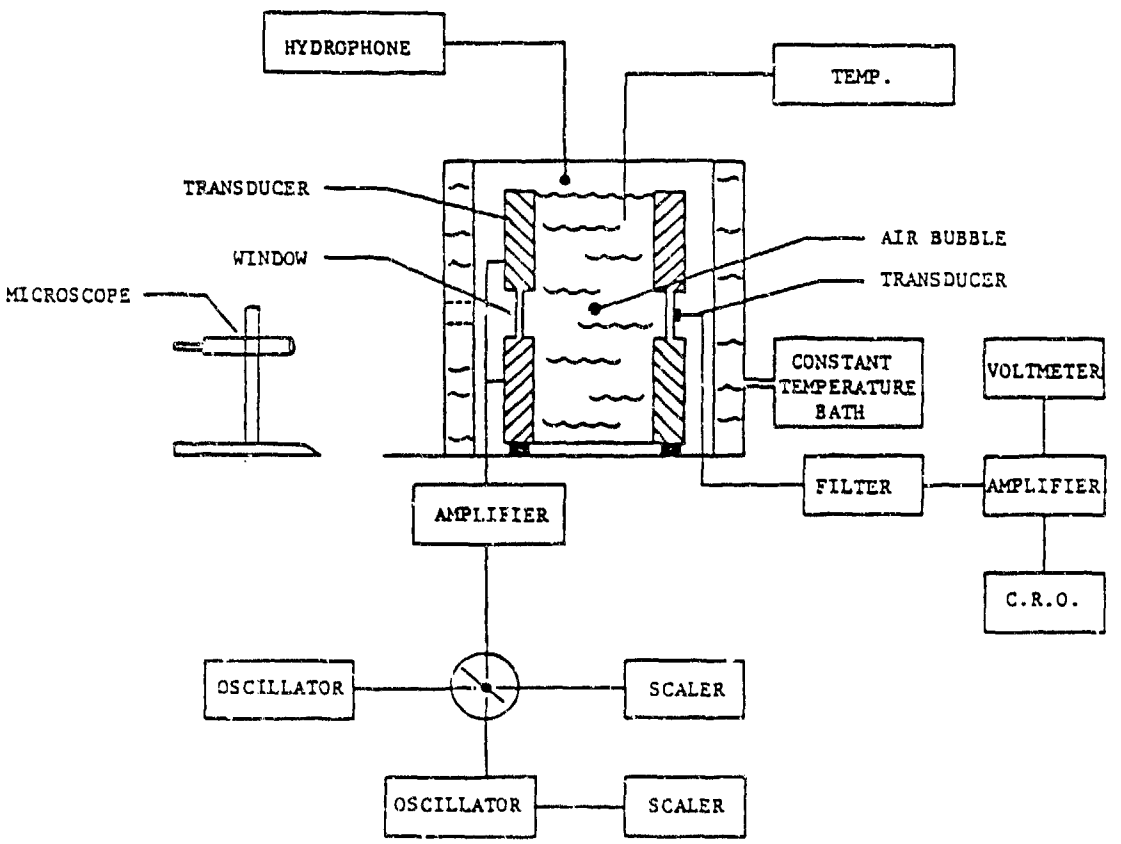

Fig. 8. Diagram of experimental apparatus for use in rectified diffusion measurements.

exists positions of stable equilibrium for the bubble in the "levitation chamber" somewhat above the position of the pressure antinode. With a little practice, one can easily position a bubble within the field and monitor this position with a cathetometer.

The normal approach is then to establish a fixed acoustic pressure amplitude within the chamber, which essentially fixes the position of the bubble (the position is independent of the radius if the bubble is sufficiently smaller than resonance size). The radius is then measured with some technique (such as permitting the bubble to rise at its terminal velocity, measuring this velocity and then determining the radius from an applicable drag law) as a function of time. For threshold measurements, the acoustic pressure amplitude is constantly adjusted to ascertain the value for which a bubble of measured size neither grows nor dissolves.

With this technique it appears that threshold measurements can be made to within an accuracy of approximately 5%. The radii measurements depend upon the applicability of the drag law, and its specific accuracy, but are probably good to within a few percent also.

E. Some Experimental Results

In this section is presented a graphical representation of the equations as a function of the various physical parameters that are applicable. Some measurements of thresholds and bubble growth rates are also given for comparison. In these figures, unless specific mention is made otherwise, it is assumed that we are considering an air bubble in water with the following set of experimental conditions: $P_\infty = 1.01 \times 10^5$ dyn cm^{-2}, $\sigma = 68$ dyn cm^{-1}, $\rho = 1.0$ g cm^{-3}, $D_1 = 0.20$ cm^2 s^{-1}, $\mu = 1.0 \times 10^{-2}$ g cm^{-1} s^{-1}, $c = 1.48 \times 10^6$ cm s^{-1}, $\gamma = 1.4$, $T = 293$ K, $D = 2.4 \times 10^{-5}$ cm^2

s^{-1} and $d = 2.0 \times 10^{-2}$.

It is seen from (36) that the numerator of threshold equation can be made to equal zero if the gas concentration ratio $C_i/C_o = 1 + 2\sigma/R_o P_\infty$. That is, if the liquid is oversaturated by an amount greater than the surface tension term, gas bubles will grow with no acoustic field applied. This important fact will be discussed in some detail later.

Consider Fig. 9, which shows a plot of bubble radius against the dissolved gas concentration ratio (C_i/C_o) for various surface tensions such that the 'critical saturation' condition is met, that is, $C_i/C_o = 1 + 2\sigma/R_o P_\infty$. This figure is presented to show the importance of the dissolved gas concentration on gas bubble stability.

Central to the study of rectified diffusion are measurements of the acoustic pressure amplitude required for bubble growth and the agreement between these measurements and the applicable theory. Shown in Fig.10 are measurements of the threshold for a region (i) case (frequency 22.1 kHz, bubble radii ranging from 20 μm to 70 μm) along with the theoretical calculations. The solid curve is the prediction of (36); the dashed line is a simplified version of the threshold applicable to this region of consideration [73]. It is seen that the two equations give similar predictions until the bubble radius becomes so small that the term $2\sigma/R_o P_\infty$ becomes significant with respect to unity.

The agreement between theory and experiment (for this limited range of bubble radii) is seen to be rather good and within the range of experimental error. This bubble range is particularly important at this frequency because it partially bridges the gap between isothermal behavior (for $R_o = 20$ μm, $n = 1.01$) and adiabatic behavior (for $R_o = 80$ μm, $n = 1.23$) of the bubble pulsations. The gradual reduction in the threshold as the bubble radius increases is mostly due to the fact that as the bubble

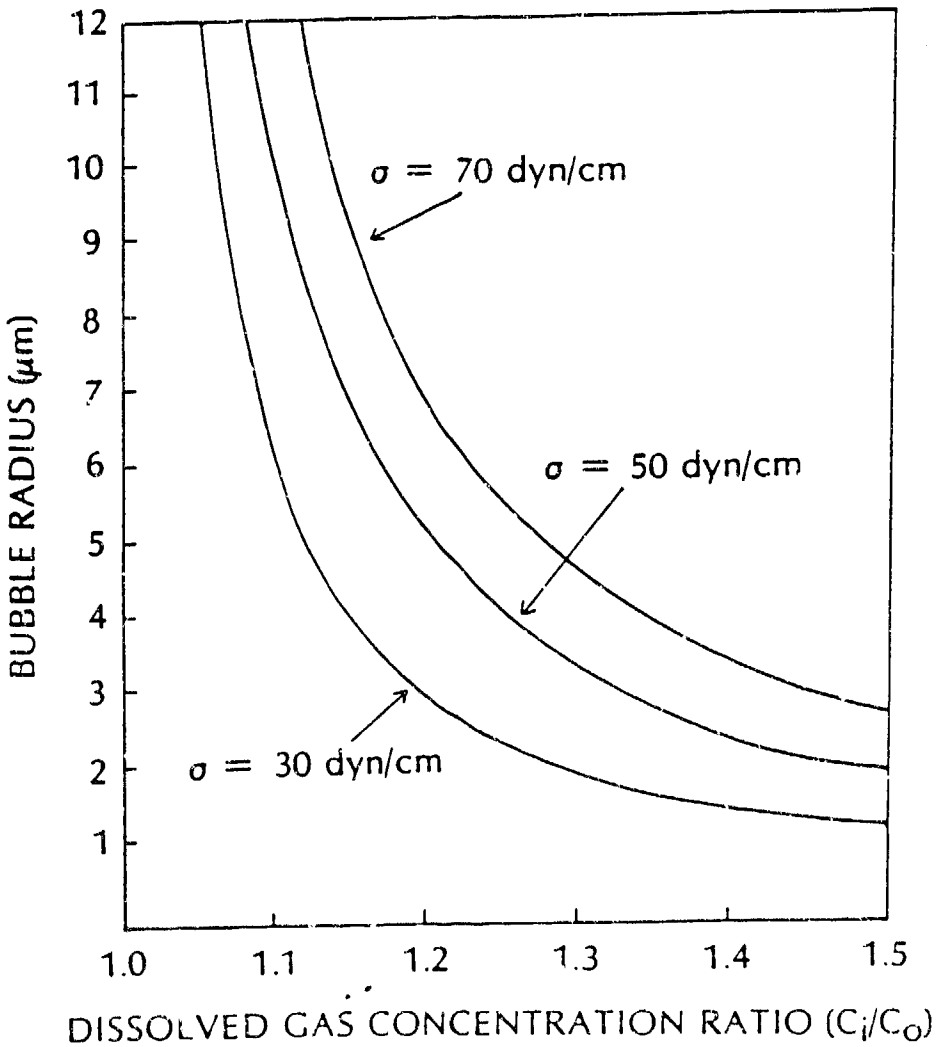

Fig. 9. Stability curves for gas bubbles at various dissolved gas concentration ratios in water. The curves are for three different surface tensions. If a gas bubble lies above the appropriate line, it will grow by diffusion at zero acoustic pressure amplitude; if it lies below, it will dissolve.

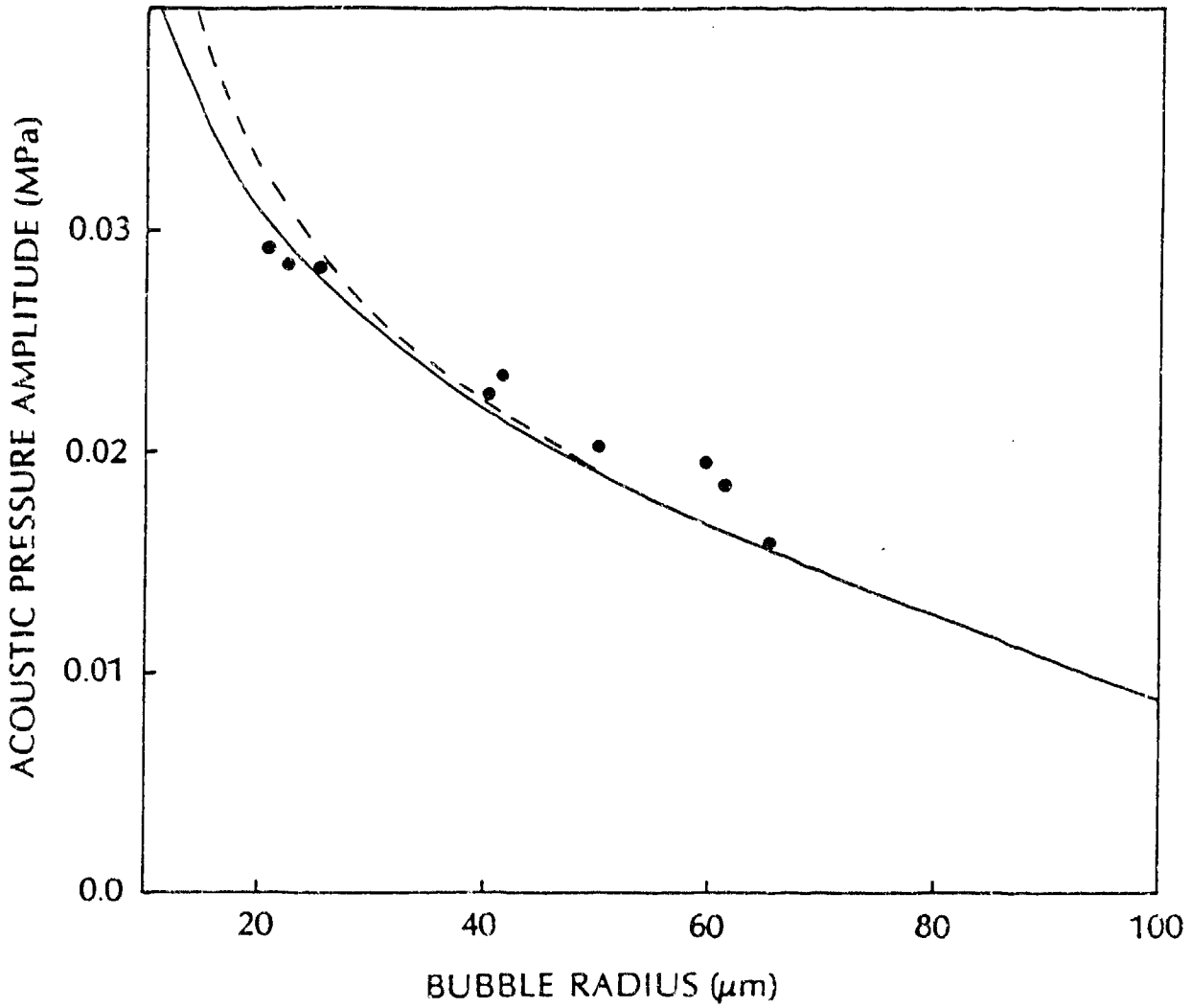

Fig. 10. Variation of the threshold for growth by rectified diffusion of an air bubble in water as a function of the bubble radius for a frequency of 22.1 kHz, a surface tension of 68 dyn cm^{-1} and a dissolved gas concentration of 1.0. The symbols are experimental measurements; the solid curve is calculated from Eq. (36); the dashed one from a less complicated expression in ref. [66].

grows toward resonance size its pulsation amplitude increases, which results in more rectified mass tranfer per cycle. Shown in Fig.11 is the variation in the rectified diffusion threshold as a function of frequency for two different values of the bubble radius.

A gas bubble present in a liquid containing a sinusoidally varying pressure field behaves very much like a damped driven harmonic oscillator. It has a linear resonance frequency given by (41). For a system in which the frequency is fixed, and the radius varies, as is typical of studies involving rectified diffusion, one can speak of a 'resonance radius' given by a solution of (41) for R_o when ω_o is replaced by the driving frequency. In Fig. 12 the driving frequency is 1.0 MHz, the surface tension 68.0 dyn cm^{-1}, and the ambient pressure 0.1 MPa, thus giving a resonance radius of 3.15 μm. It is seen that the threshold becomes very low near resonance due to the large pulsation amplitude of the bubble there. Near resonance, the amplitude of the bubble's pulsations are determined mostly by the damping, which is relatively small, and consequently the bubble oscillates rather violently. It is not expected that the equations for bubble growth and for the threshold will be very accurate in this region, however.

So far, our analysis in this section has been limited to the rectified diffusion threshold. It is in order also to examine the rate of growth by rectified diffusion when the acoustic pressure amplitude exceeds the threshold. An examination of the growth (or decay) of a bubble is shown in Fig. 13. The symbols are experimental measurements; the curves were obtained by numerical integration of (35). It was observed by Eller [57] that his measurements of the growth rate were considerably larger than predicted by theory. Gould [58] later confirmed the excessive growth rates but also noticed that surface oscillations, with their associated acoustic

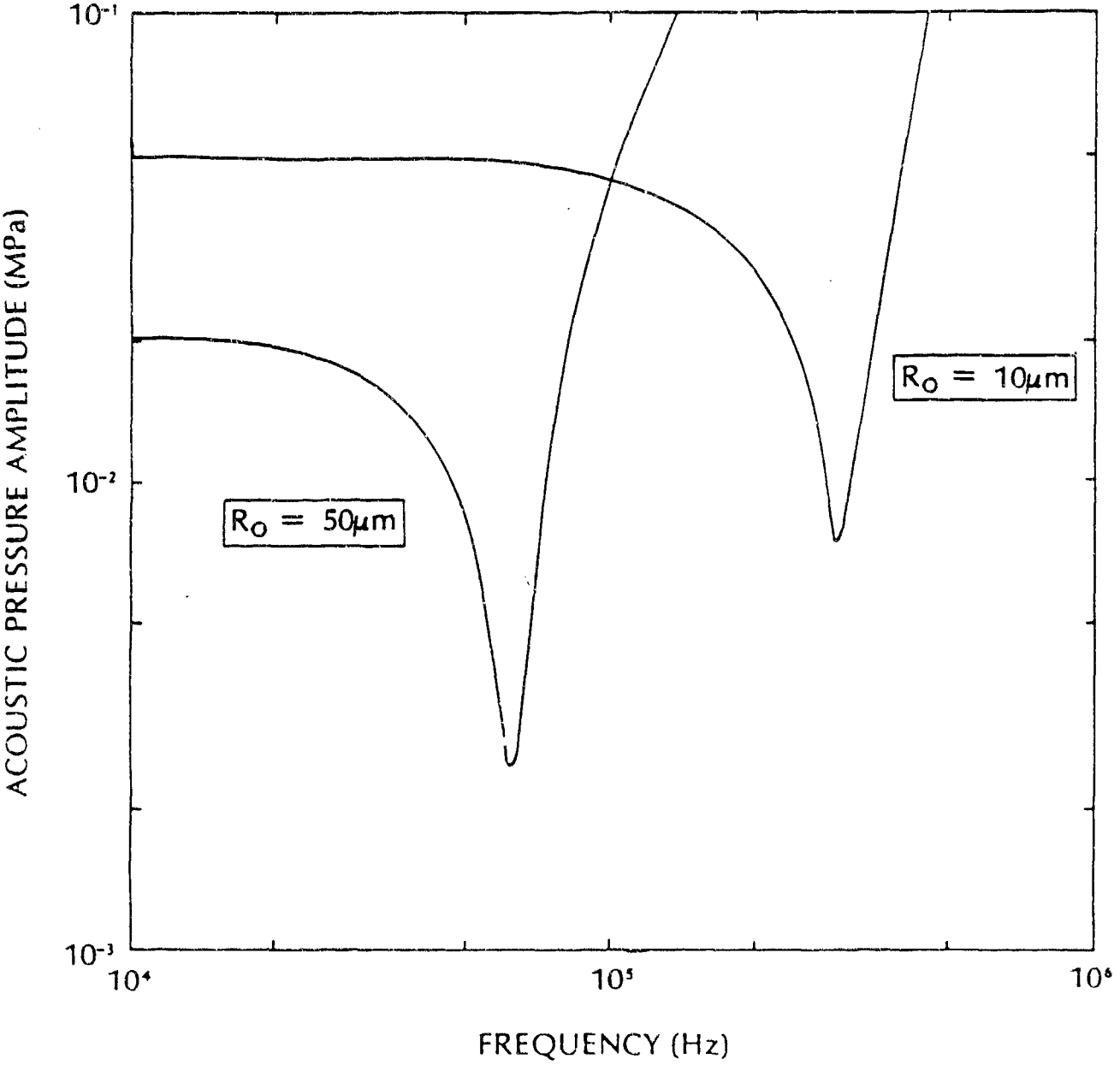

Fig. 11. Variation of the rectified diffusion threshold as a function of acoustic frequency for two different values of the gas bubble radius. The liquid is assumed to be water having a dissolved gas concentration ratio of 1.0 and with a surface tension of 68 dyn cm^{-1}.

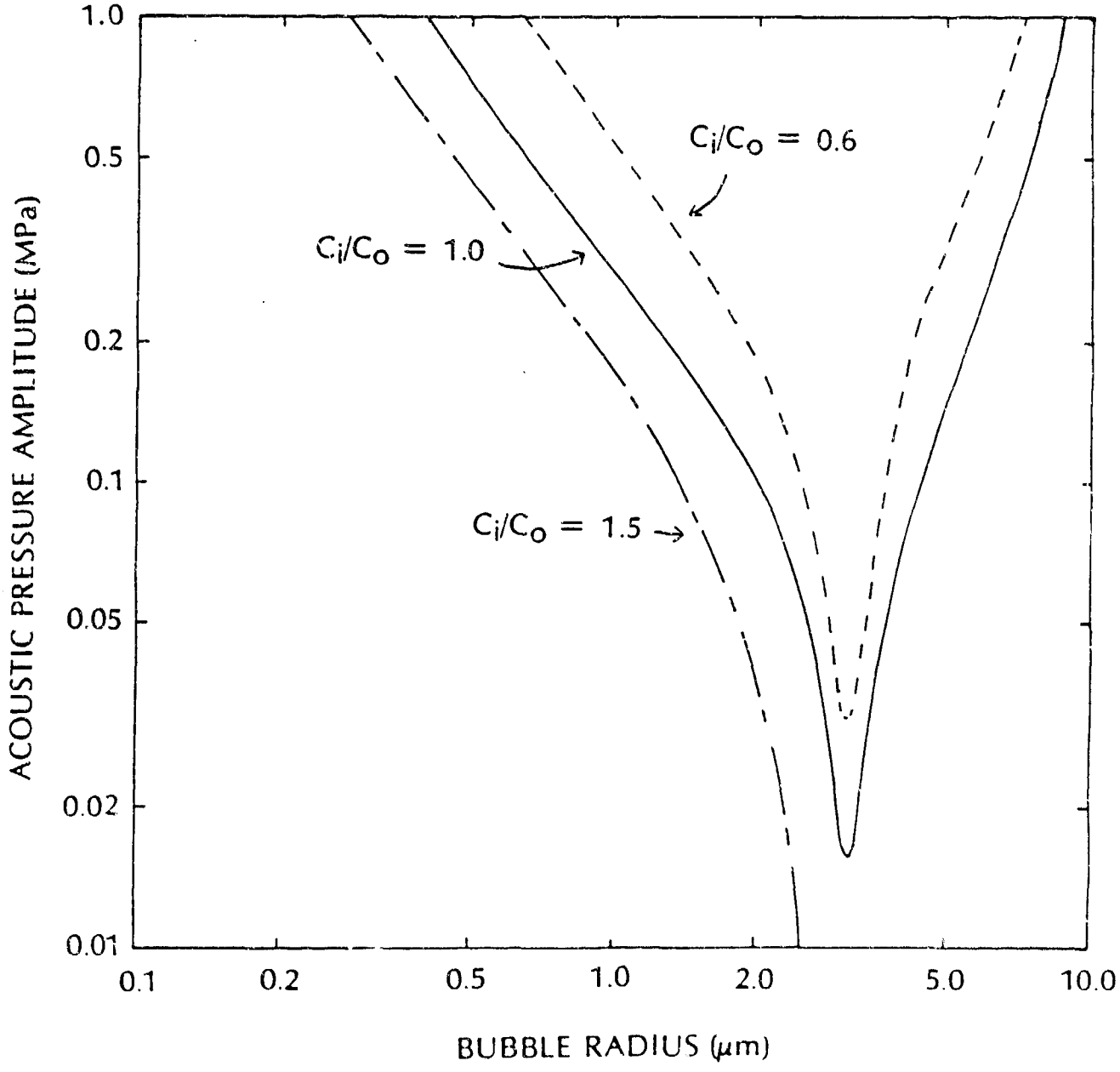

Fig. 12. Variation of the rectified diffusion threshold as a function of gas bubble radius for three separate dissolved gas concentration ratios (C_i/C_o). The curves can be calculated by the use of Eq.(36); the acoustic frequency used was 1.0 MHz and the surface tension was 68 dyn cm^{-1}; the liquid is assumed to be water.

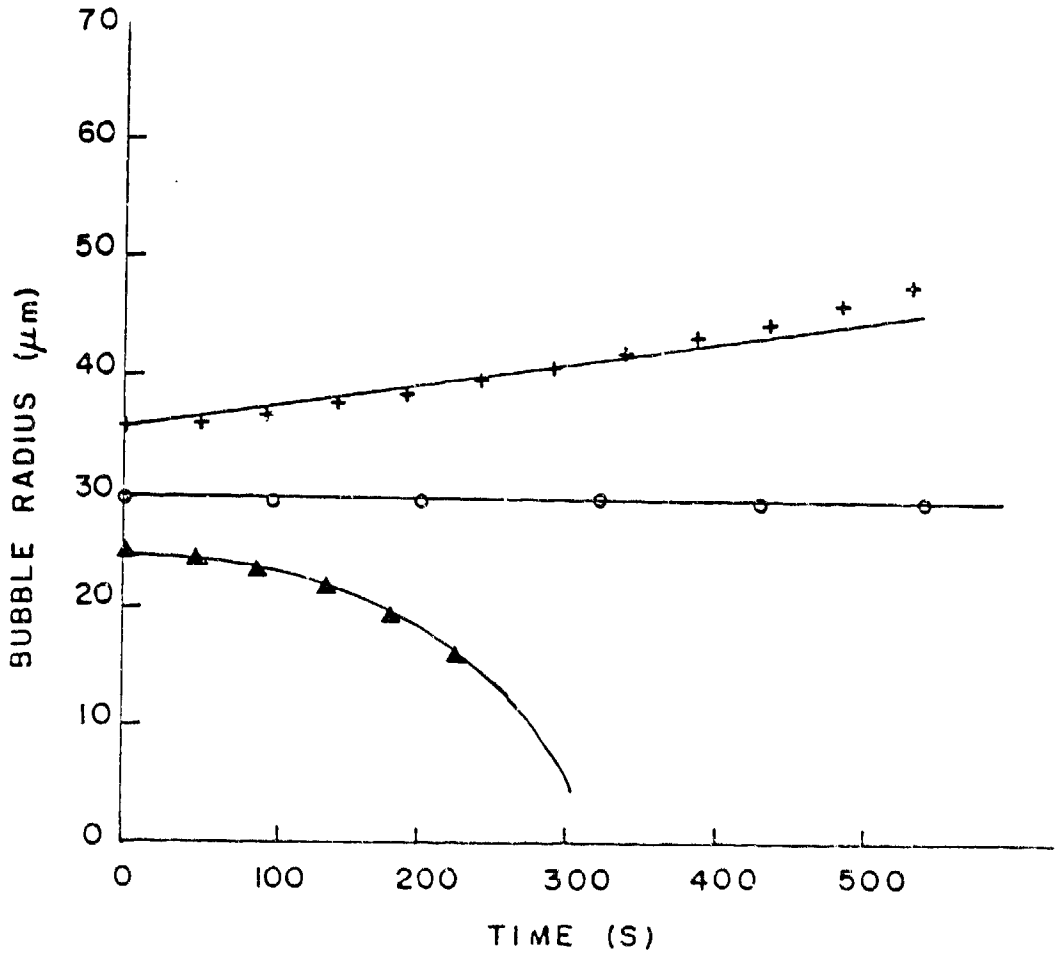

Fig. 13. Variation of the bubble radius with time for a liquid surface tension of 68 dyn/cm and an acoustic pressure amplitude of 0.27 bar. The liquid was saturated with gas. The solid lines are calculated by numerical integration of Eq. (35).

streaming, were probably the explanation for the increased growth rates that he observed.

Shown in Fig.14 are some observations of growth rates made by Crum [63]. He observed an agreement between the measured and predicted rates provided surface oscillations were avoided, and provided that the water was relatively pure and free of surface-active contaminants. When surface-active agents were added to the water, growth rates much higher than predicted were observed. Among the explanations offered for this effect were that (a) the surface active agents were behaving as a rectifying agent, permitting more diffusion in than out, and (b) acoustic streaming was occurring in the absence of surface oscillations, induced somehow by the surface contamination. This interesting anomaly has not yet been explained.

Our attention is now turned to cases that are more applicable to biological systems. As a specific experiment to consider, it was demonstrated by ter Haar et.al. [25-26] that echo centers probably representing gas bubbles were observed in live guinea pig legs when exposed to therapeutic ultrasound. It was suggested by Crum and Hansen [65] that these bubbles of observable size were the result of cavitation nuclei that were made to grow by rectified diffusion. Consider Fig. 15 which demonstrates what would happen to a population of free air bubbles (that are unstabilized) with radii varying from 1μm to 2 μm present in water when exposed to continuous wave ultrasound of frequency 3 MHz and acoustic pressure amplitude of 0.12 MPa. This figure may be applicable to the growth of microbubbles in tissue by therapeutic ultrasound. Note that if this population of 'free air bubbles' were suddenly created, those bubbles with radii less than 1.03 μm would slowly dissolve regardless of the ultrasound. Those bubbles in the range of 1.03 μm to 1.4 μm would grow to

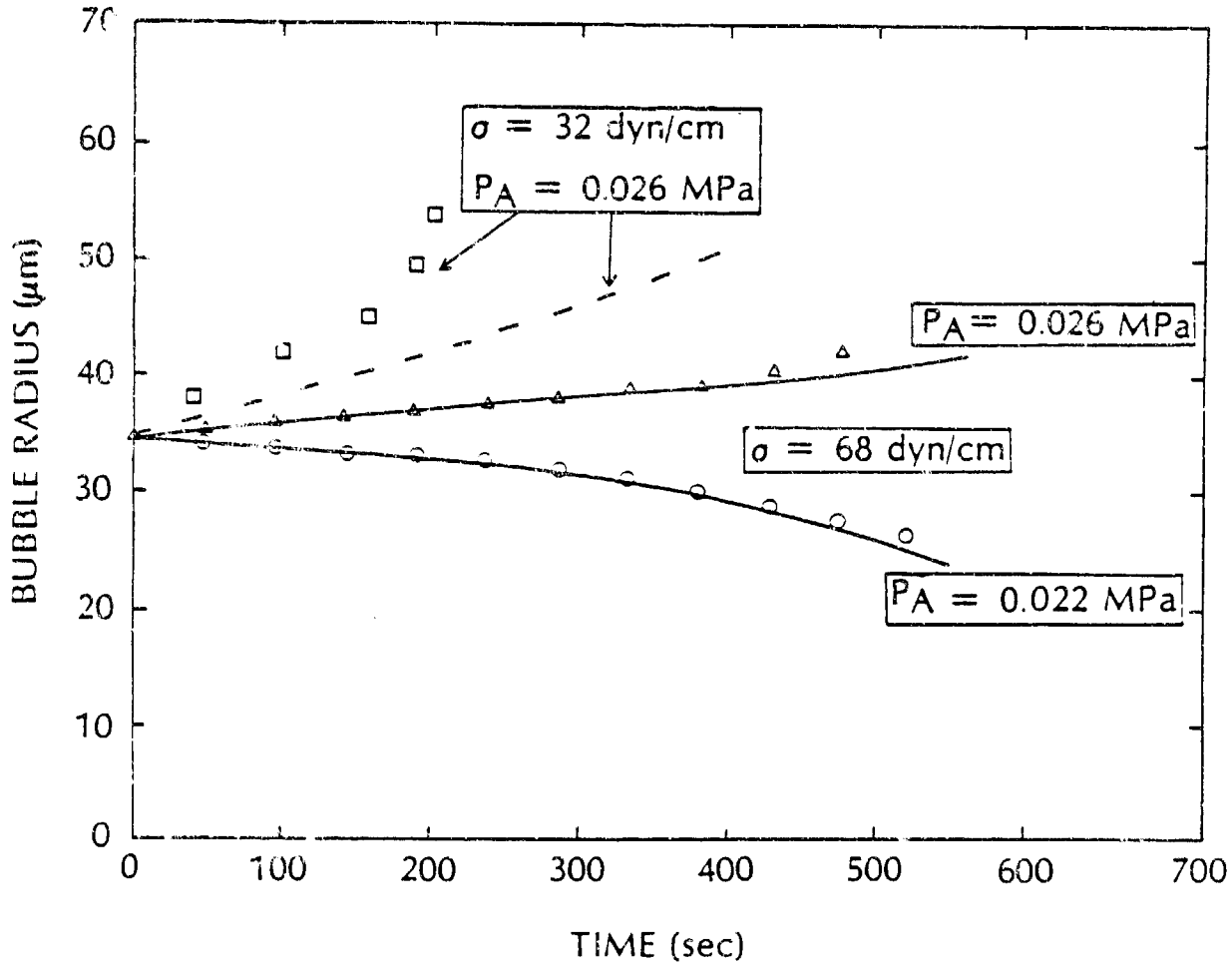

Fig. 14. Dependence of the bubble radius on time for an air bubble undergoing rectified diffusion in water. The symbols are measured values; the curves have been calculated by numerical integration of Eq. (35). The bottom two curves (and measurements) are for distilled water having a surface tension of 68 dyn cm^{-1}; the top curve (and associated set of measurements) is for water containing small amounts of surface-active agents, and having a surface tension of 32 dyn cm^{-1}.

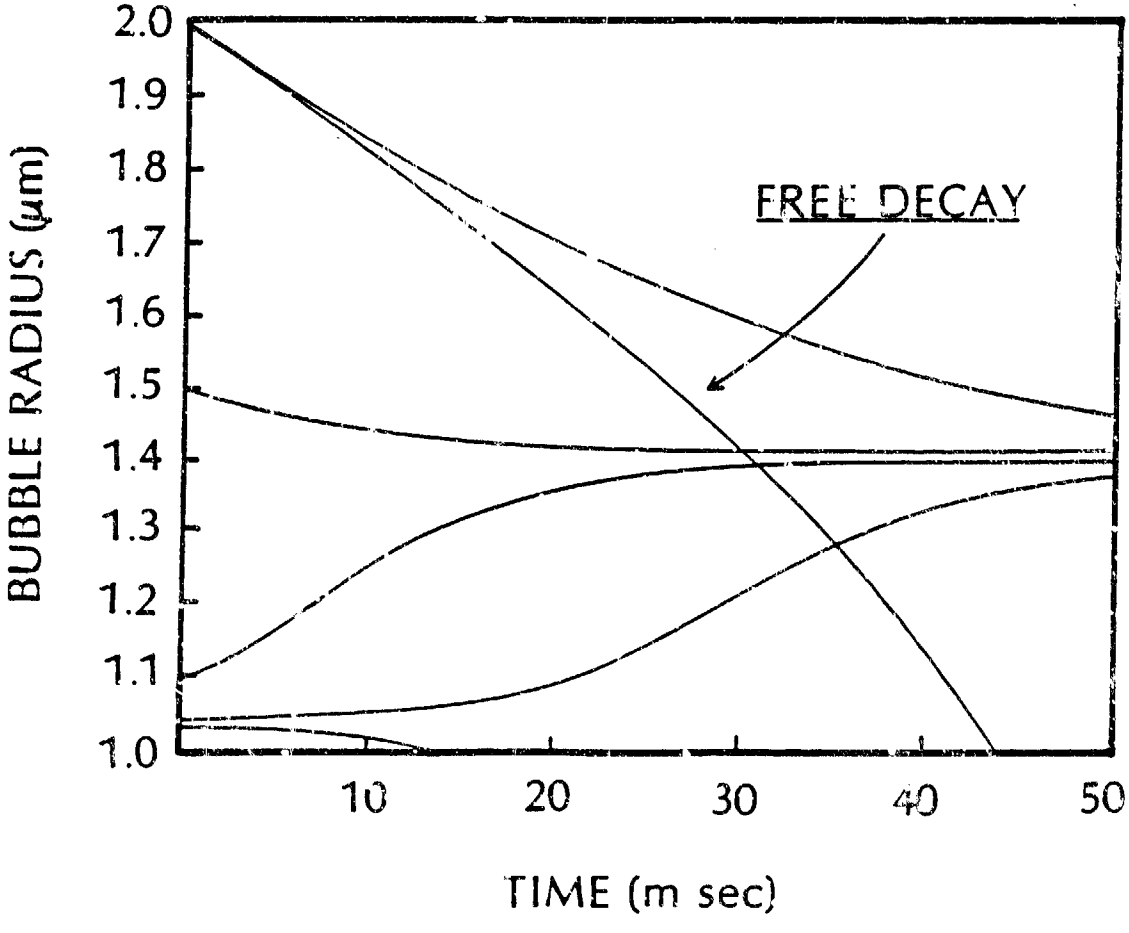

Fig. 15. Calculated behavior of a distribution of the sizes of air bubbles present in water as a function of time and exposed to a continuous sound field of frequency 3.0 MHz and acoustic pressure amplitude of 0.12 MPa. The designated line indicates the free decay of an air bubble. The other lines describe the time history of individual air bubbles and were obtained from a numerical integration of Eq. (35).

an asymptotic limit of about 1.42 μm. Bubbles larger than 1.4 μm would decay to the asymptotic limit.

The reason for this limit is that due to the Laplace pressure, there is always a tendency to force gas out of the bubble (note the free decay curve on the figure). If the bubble radius is less than resonance size, and greater than a threshold size, the bubble will grow through resonance to a size sufficiently above resonance where its pulsation amplitude will result in an inward mass transfer due to pulsation that just matches the outward mass transfer due to the Laplace pressure. If the bubble is larger than the asymptotic limit, it will not be able to overcome the outward diffusion due to the Laplace pressure and will dissolve slowly until its pulsation amplitude is large enough to stop further dissolution. Consequently, there is a tendency to force microbubbles present in a liquid to a uniform size that is dependent on the intrinsic and extrinsic physical parameters.

The discovery by ter Haar et. al. that bubbles could be made to grow in vivo by the action of CW ultrasound is extremely important in our study of the bioeffects of ultrasound. Since it was seen in Fig. 15 above that gas bubbles would be forced to grow toward an asymptotic limit, it is possible to use this concept to explain the presence of the bubbles that they observed.

The results of the experiment performed by ter Haar et.al. is depicted graphically in Fig. 16. In that experiment they irradiated an anesthesized guinea pig with therapeutic ultrasound while monitoring the irradiated area with a diagnostic scanner that could detect objects such as bubbles down to a minimum size of 10 μm in diameter. Fig. 16 shows that the cumulative number of events observed as a function of irradiation time for four values

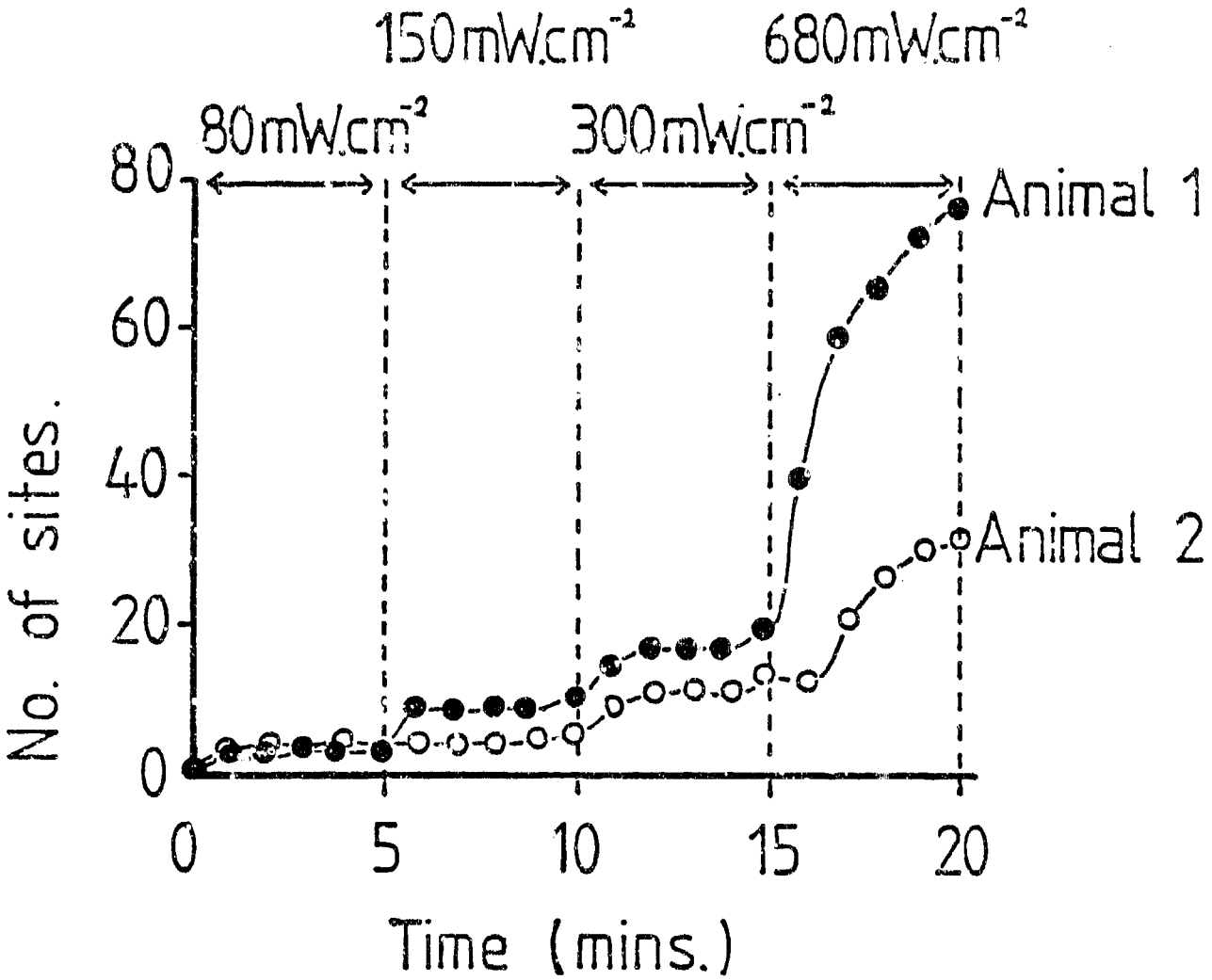

Fig. 16. Rate of accumulation of sites of bubble formation during irradiation with 0.75 MHz ultrasound plotted as a function of time and intensity. Results from two different animals are shown.

of the spatial average intensity. The bubbles were assumed to have diameters larger than 10 μm as that value was the approximate limit of their resolution.

These data were analyzed by Crum and Hansen [65] and an explanation given in terms of growth of cavitation nuclei by rectified diffusion. Fig. 17 shows the results of their calculation of the growth of nuclei (assumed to be free bubbles) to sizes greater than the resolution limit for the various intensities used in the ter Haar study (note that temporal peak intensities were used in the calculation because the bubbles respond to the peak acoustic pressure rather than the spatial average pressure - they are very small compared to the diameter of the irradiating transducer). It is seen that only a few nuclei grow to visible size for the lowest intensities; in agreement with the observation of ter Haar et.al. The fact that bubbles were seen that were larger than the theoretical asymptotic limit is explained as due to bubble coalescence by Bjerknes forces [65].

F. Observations and Comments

The observations about rectified diffusion that appear applicable to a biological interests are as follows:

(i) pulsating bubbles are dynamic systems: A gas bubble present in a CW sound field will grow in size if driven with a pressure amplitude that is larger than the threshold for rectified diffusion. As the bubble grows it will pass through harmonic regions [74] where its pulsation amplitude can become very large inducing in turn severe shear stresses [42] in the vicinity of the bubble. These shear stresses have been calculated by Bjorno and Lewin to be sufficient to cause biological damage [41].

(ii) rectified diffusion thresholds can be exceeded by therapeutic ultrasound devices: The fact that ter Haar et.al. [25] have seen hundreds of bubbles produced by therapeutic ultrasound devices coupled with the

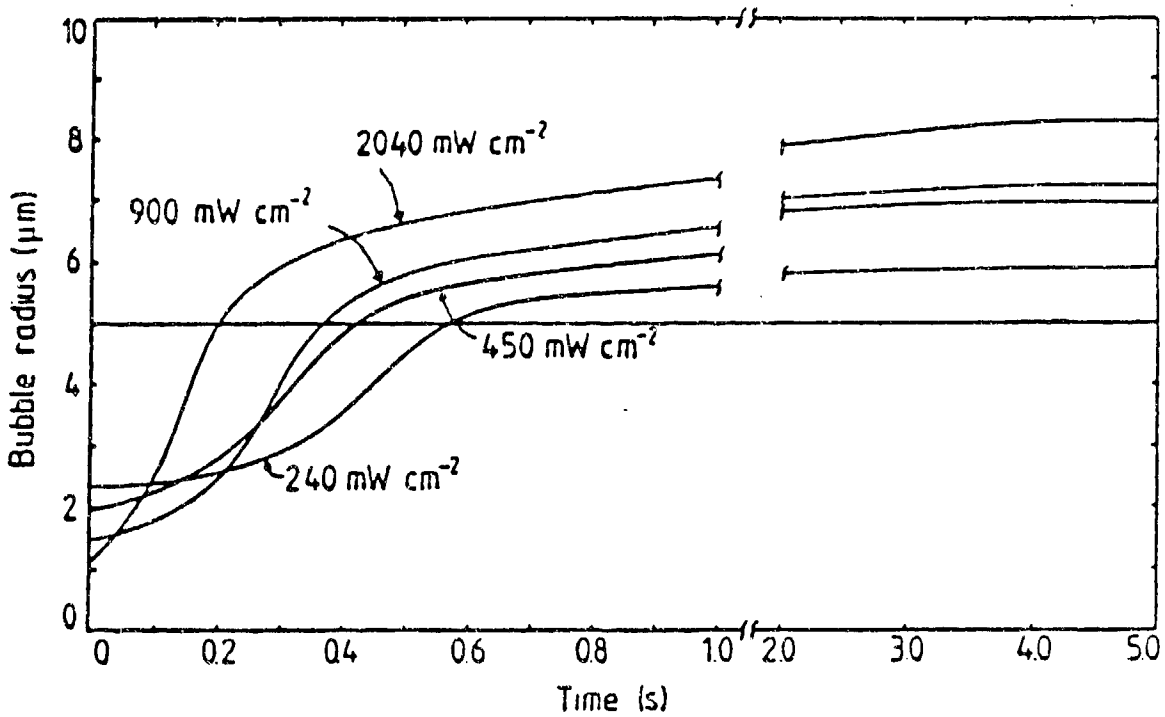

Fig. 17. Growth of air bubbles by rectified diffusion from a threshold radius to maximum size. The four curves are for the four different intensities used in the ter Haar and Daniels study (temporal peak intensity is given here). The heavy line indicates the approximate minimum size for which the bubbles can be detected with the pulse-echo system. These curves are for a frequency of 0.75 MHz, a surface tension of 60 dyn/cm and a gas concentration level of 1.0.

observaion by Crum and Hansen [65] that this growth is consistent with the predictions of rectified diffusion leads us to believe that this type of behavior has a widespread occurrance. Recent studies by Dyson [75] that healing rates can be significantly improved by application of therapeutic ultrasound give additional evidence to this contention. In both ter Haar's and Dyson's experiments, the application of a few atmospheres of static pressure essentially eliminates the effects. Obviously bubbles are involved; the mechanism of rectified diffusion is a likely candidate for the explanation of the observations.

(iii) <u>stabilized nuclei may have significantly lower rectified diffusion thresholds</u>: It was observed in the above discussions that there is a threshold for rectified diffusion because one needs to overcome the tendency of surface tension forces to force the gas contained within a bubble into solution. However, the fact that cavitation nuclei are stabilized implies that this surface tension force is somehow already balanced. In the ionic skin model of Aculichev [6] and the organic skin model of Yount [12], a pulsation that did not break up the skin would cause bubble growth essentially without a threshold. Some experimental support for this concept exists in that Crum [63] has found that the addition of surfactants to water both lower the threshold and increase the growth rate. On the other hand, since a threshold <u>does</u> exist in water, these models probably need some modification to account for the presence of the threshold. Perhaps, in water, a crevice model is required, with ionics and organics on the surface! Within biological tissue, however, it is quite logical to assume that the small pockets of gas that do exist are stabilized by mechanisms that effectively eliminate the surface tension and thus reduce significantly the threshold for rectified diffusion.

III. STABLE CAVITATION

A. Introduction

There are many areas associated with the biological effects of ultrasound in which the amplitude of the acoustic field is relatively low and the irradiation is continuous. Examples of such applications are some doppler scanners, and a variety of therapeutic devices. For these situations, a preexisting cavitation nucleus may be nucleated according to the conditions specified in section I, grow by rectified diffusion according to the equations of section II, and pulsate violently for several cycles - which we shall define as "stable" cavitation and now discuss in some detail.

B. Some governing equations

The general topic of bubble dynamics is rather broad, will probably be treated elsewhere in this course, and is beyond the scope of much of what we wish to do here. Nevertheless, we shall need to do some mathematical analysis to obtain the equations we wish to utilize.

Consider a spherical bubble present in an infinite liquid and subject to an oscillating pressure field. Following Prosperetti [76] who leans heavily on the work of Keller [77], the following equation for the radial oscillation of a bubble of instantaneous radius R(t) is obtained

$$(1-\dot{R}/c)R\ddot{R} + 3\dot{R}^2(1-\dot{R}/3c)/2 = (1 + \dot{R}/c)(p_i(R,t) - p_s(t))/\rho + (R/\rho c)\, dp(R,t)/dt. \qquad (42)$$

Here c is the velocity of sound, the dots denote differentiation with respect to time, p_i is the internal pressure, P_s is the static pressure plus the applied oscillating pressure and p is the pressure in the liquid

just outside the bubble. The internal pressure is connected to the external pressure by the condition on the normal stresses, viz.,

$$p_i(R,t) = p(R,t) + 2\sigma/R + 4\mu\dot{R}/R. \tag{43}$$

Again, σ is the surface tension and μ the viscosity of the liquid. The viscous damping term is included in (43) and not in (42) partly out of convenience and mostly because it can be quite significant for very small bubbles. Eq. (42) contains the effect of the compressibility of the liquid and does not make the polytropic exponent approximation. If the liquid is assumed to be incompressible and the polytropic approximation is made, then the well-known Rayleigh-Plesset equation, given earlier as Eq. (16), is obtained. It will be desirable to use (42) in some of our calculations to be discussed below rather than (16).

For the time being, however, let us assume that the polytropic exponent approximation can be made and examine solutions to the Rayleigh-Plesset equation that will enable us to describe the oscillations of a gas bubble driven at relatively low pressure amplitudes.

The linear or first-order approach to this problem is to assume that the radius of the bubble can be written as

$$R = R_o (1 + x). \tag{44}$$

where x is given by Eqs. (22) through (26). This approach enables one to obtain an analytical expression that closely approximates the threshold and growth rate for rectified diffusion, as shown earlier in Figs. 10 and 13, and enables one [78] to indirectly measure the variation of the polytropic exponent with bubble radius, as shown in Fig. 18. This figure shows that the linear approximation described above gives a general description of the variation of the polytopic exponent with the bubble radius until the ratio of bubble size to rsonance size approaches the value 0.5. At this point,

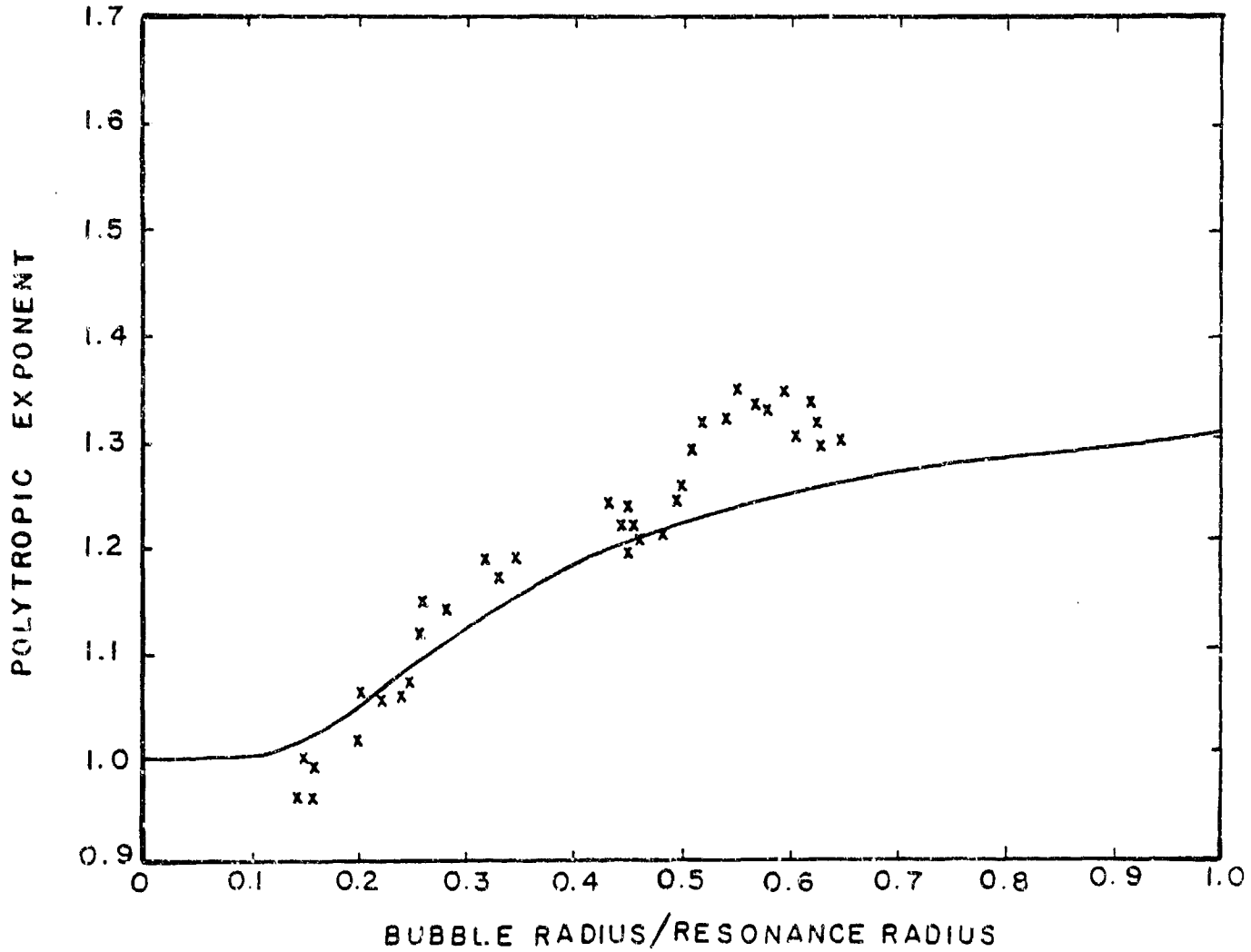

Fig. 18. Variation of the polytropic exponent with bubble radius for air bubbles in water. The symbols are experimental measurements and the solid line calculated from the equations obtained independently by Eller [68] and Prosperetti [67]. For this case, the acoustic frequency was 27.2 kHz, the surface tension 68 dyn/cm and the resonance radius 158 μm.

the second harmonic resonance of the bubble is excited and the agreement between the linear theory and the experimental measurements fails. Of course, this is only one of the many harmonic resonances; at other sites, the linear theory will also fail if the amplitude of the radial oscillations is sufficiently large.

C. Nonlinear behavior of the bubble.

This failure demonstrates an important caveat that must be acknowledged when dealing wih the oscillations of a gas bubble in a liquid: a pulsating gas bubble is a highly nonlinear system and its nonlinear behavior can be activated at very low values of the acoustic pressure amplitude. For example, the average acoustic pressure amplitude required to introduce these nonliner effects in Fig. 18 was on the order of 0.25 bar (0.025 MPa).

To follow up on this point, consider Fig. 19 which is a plot of the relative pulsation amplitude, $X_m = (R_{max} - R_o)/R_o$, versus the ratio of the driving frequency to the resonance frequency for a 1.0 μm bubble in water. The figure shows the results of a numerical calculation by Lauterborn [79] and an approximate analytical solution by Prosperetti [74] of the Rayleigh-Plesset equation. Note that a smooth linear resonance curve is not observed; there is, in fact, considerable nonlinear structure in the form of higher harmonics. The amplitude of these higher harmonics can be quite considerable. Some experimental confirmation of these results are shown in Fig. 20. This plot shows the variation of the Levitation Number, a useful nondimensional number [80, 81] that is quite similar to the X_m of Lauterborn and Prosperetti, plotted versus the ratio of the measured radius to the resonance radius (approximately equal to ω/ω_o) for an air bubble in a glycerine/water mixture. The experimental points show that this

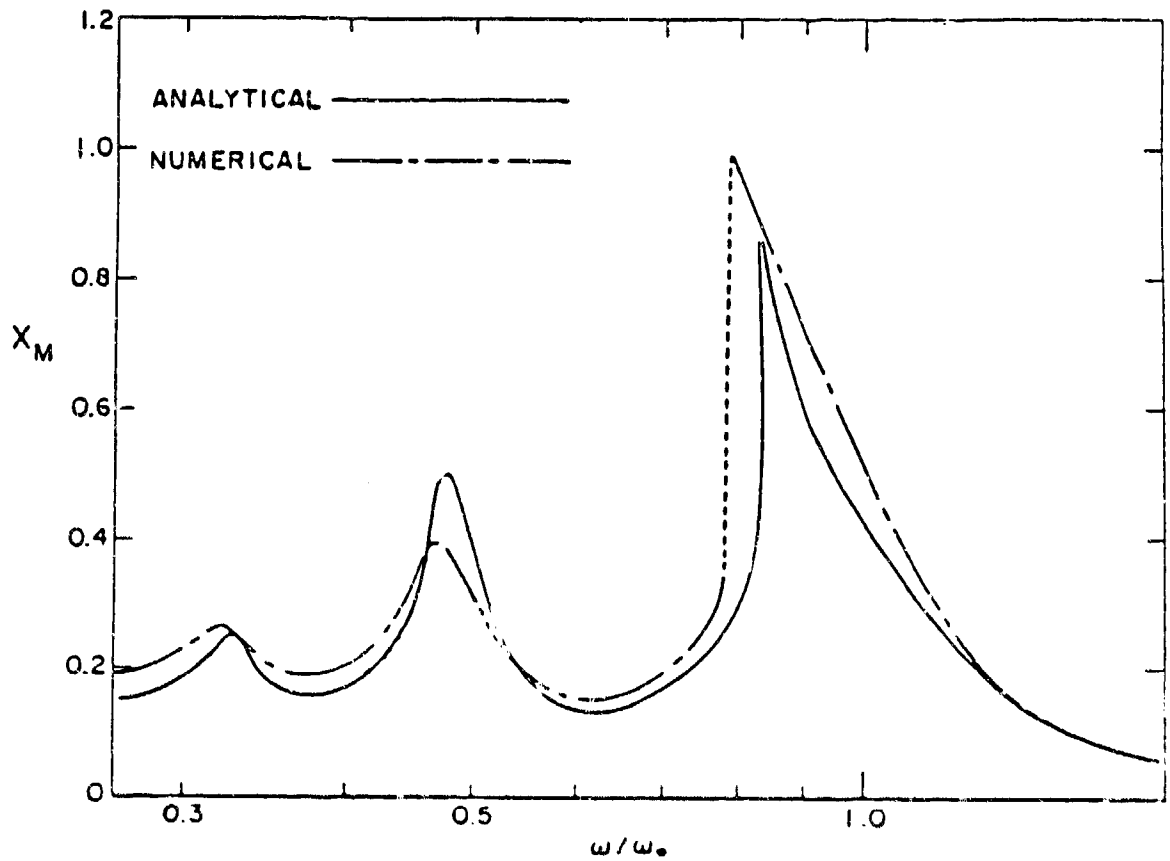

Fig. 19. Variation of the relative pulsation amplitude with normalized frequency for a 1.0 micron bubble in water. For this case, the acoustic pressure amplitude was 0.9 bar and the two curves represent analytical and numerical estimates of the bubble response. Note the highly nonlinear behavior.

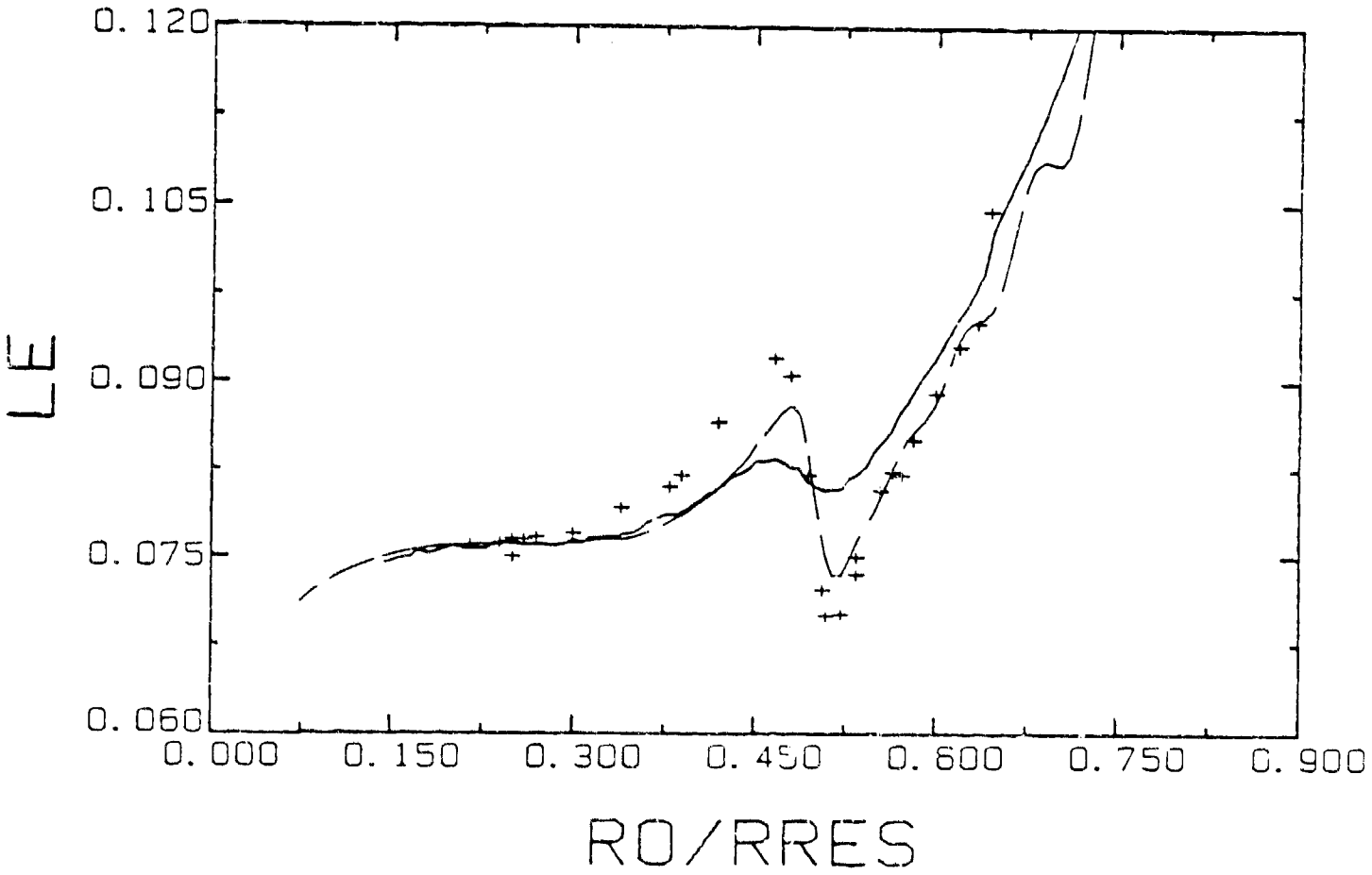

Fig. 20. Variation of the Levitation number with normalized bubble radius for an air bubble in a glycerine/water mixture. The solid line represents a numerical solution to Eq. (16) with use of a polytropic approximation and an "effective viscosity" used to account for the thermal damping. The broken line represents a naumerical solution to Eq. (42) with the thermal damping calculated directly from the internal pressure. The symbols are experimental measurements. For this case, the driving frequency was 22.2 kHz and the resonance radius was 138 microns.

nonlinear behavior is easily observed; the drawn lines are theoretical calculations that indicate that there is not good agreement between the calculated and measured values. The solid line shows the analytical result that one would expect if one assumes a polytropic approximation; the broken line is a numerical result in which the internal pressure is calculated directly, and the thermal damping obtained from this result. In this recent calculation, we have used Eq. (42) and obtained the internal pressure by a solution of the Navier-Stokes equations [82]. This new formulation is quite fundamental in approach and gives us an opportunity to examine a host of interesting problems of this nature in the future.

D. Harmonics, subharmonics and noise.

One anticipates that the sound radiated by an oscillating bubble will be related to the radius-time curve of a bubble's oscillation for a given set of physical parameters. We have shown that most aspects of nonlinear bubble dynamics can be described (in a qualititive sense, at least) by analytical and numerical approaches. We show in Fig. 21 the radius-time (R-t) curve that was obtained numerically for a bubble under the given conditions shown on the figure. This result was obtained by a numerical integration of the Rayleigh-Plesset quation, Eq. (16). Also shown in Fig. 21 in the upper left-hand corner, is a frequency spectrum of that bubble's oscillation. Note that the bubble's R-t curve shows obvious nonlinear effects that are detailed more clearly in the frequency spectrum (hereafter referred to as the Fast Fourier Transform, FFT). It is seen that with the given conditions, the frequency spectrum is rich in harmonics, but shows only an indication of subharmonic behavior. We shall assume (somewhat naively) that the sound radiated from the bubble would reflect the composition of the FFT. By the way, our numerical solution given in Figs. 21 and 22 includes our best estimate of intrinsic bubble parameters such as

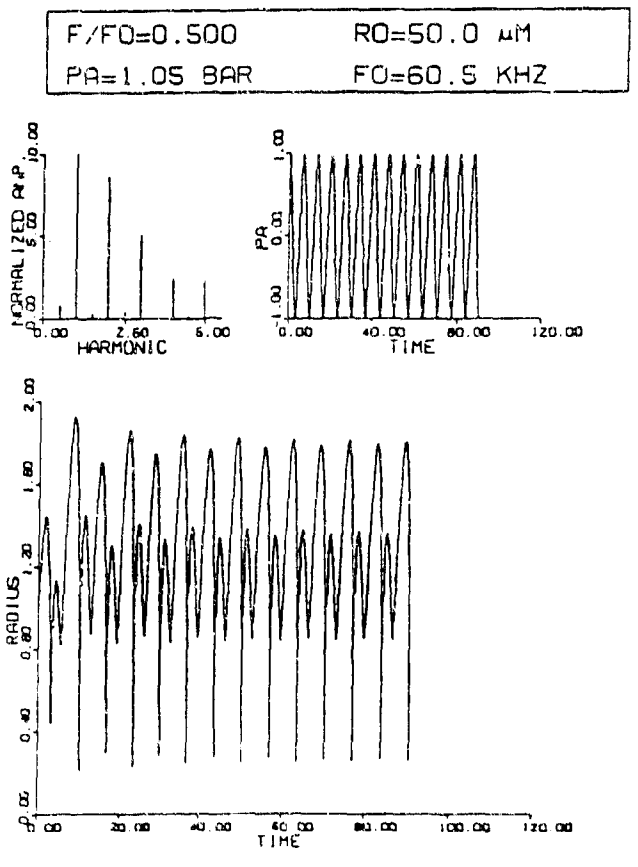

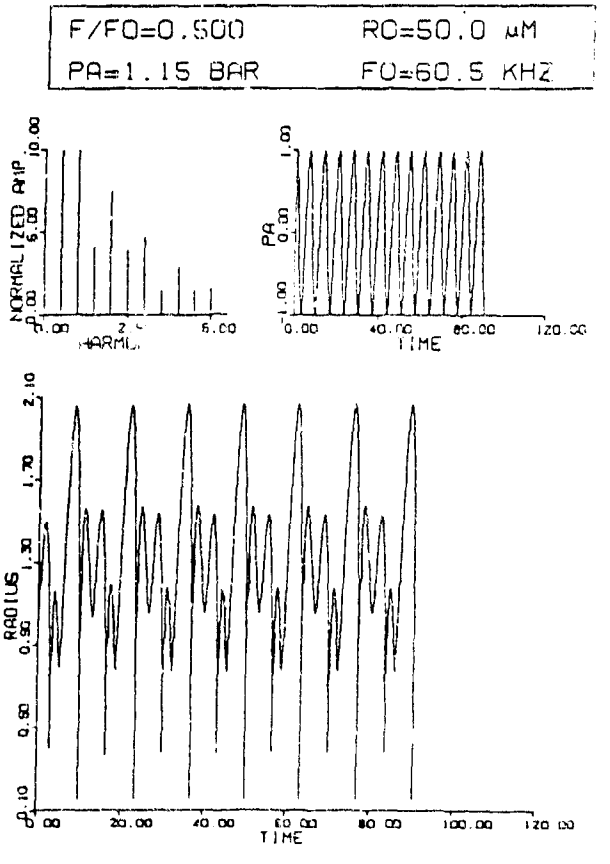

Figs. 21 (left) and 22 (right). Radius-time curves and frequency spectrum plots for a gas bubble oscillating under the conditions given in the headings. Note that a small change in acoustic pressure amplitude causes a significant increase in the subharmonic response. Note also the change from period one to period two behavior.

the damping and the polytopic exponent.

A very important aspect of our still preliminary results is shown in Fig. 22. This figure reflects the same conditions shown in Fig. 21 except that the acoustic pressure amplitude has been increased by approximately 10%.

The FFT now shows that the bubble's oscillation is rich in subharmonics and ultraharmonics ($3f_o/2$, $5f_o/2$ etc.). The rapid appearance of these frequency components implies that a threshold exists for their generation and that once they appear the spectrum can rapidly approach what one can term white noise. We can show this idea by taking a slight digression to consider what is commonly called the theory of "deterministic chaos".

E. Bubble Chaos

It can be observed in Fig. 21 that in the R-t curve, there is an obvious transient response that rapidly leads to steady-state behavior. The steady state that the bubble may approach may be a simple linear response that oscillates at the driving frequency, or, if the driving amplitude is sufficiently high, at a frequency that is half the driving frequency (subharmonic of order 1/2), or a frequency that is twice the driving frequency (harmonic of order 2), or any number of other allowed frequencies. Consider a phase-space plot of the velocity of the bubble's interface versus the radius of the bubble (often called a Poincarè Plot) as shown in Fig. 23. This plot is generated by examining a constant-phase value of the radius and the velocity after each cycle. In this case, the bubble was driven at an amplitude sufficiently high to cause it to oscillate in a "period two" mode, i.e., a subharmonic of order 1/2. Further, there was only a small amount of damping supplied so that the transient existed for several cycles.

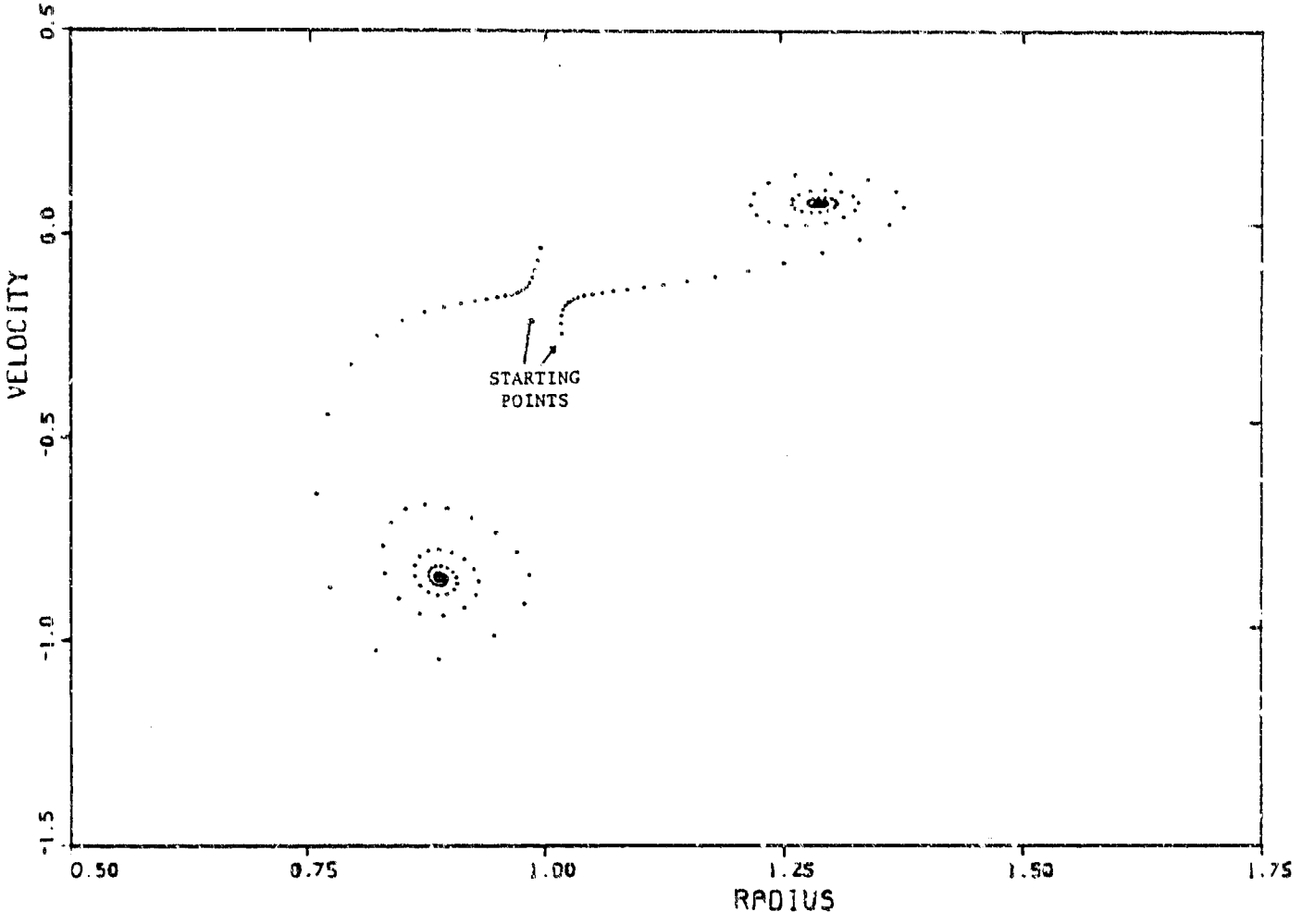

Fig. 23. Poincarè plot for a pulsating gas bubble similar to the case depicted in Fig. 22, except that for this case, the damping of the bubble pulsations is relatively small. The spirals show the movement toward the attractor locations for a period two attractor.

The two regions shoiwn on the figure show that the bubble slowly spirals into two points, called "attractors" in phase-space. If the bubble were driven at a relatively low amplitude, then it would behave linearly and spiral into only one point, and would oscillate in a "period one" mode.

We next consider what happens as the bubble is driven at progressively higher amplitudes. One method for determining what occurs is to examine the FFT. This approach is somewhat expirical in that one only observes what "has occurred", rather than following a logical, predictable path to explain what "should happen". The "chaos" approach [83-84] is to examine certain modes of oscillation in order to determine when and how the transition to chaotic behavior occurs. Consider Fig. 24 below, which we have ootained from our numerical scudies, and which describes the behavior of our nonlinear bubble system as it bifurcates to higher and higher periods. Plotted as the ordinate is the value of the radius, at some arbitrarily-fixed point in its cycle, examined as a function of driving amplitude, at the same point in the cycle. (This is as if one took a strobe picture each cycle.) Plotted as the abscissa is the driving acoustic pressure amplitude exerienced by the bubble. Note from the figure that as the amplitude is increased, there is a bifurcation from "period one" behavior to "period two" behavior at the amplitude A_1, from "period two" to "period four" at A_2 etc., until one reaches a chaotic state. Although the theory of chaos in nonlinear mechanics is still in its infancy, it has been determined that for dissipative systems (such as an air bubble), the limit of the ratio $(A_{N+1} - A_N)/(A_{N+2}-A_{N+1})$ should be given by a constant, called Feigenbaum's constant [84]. (For our system here, the value we get for this constant is 2.0, as compared to an accepted value of 4.669; however, our results are preliminary and lots of work still needs to be done. The fact that these two numbers don't agree is in itself rather interesting.)

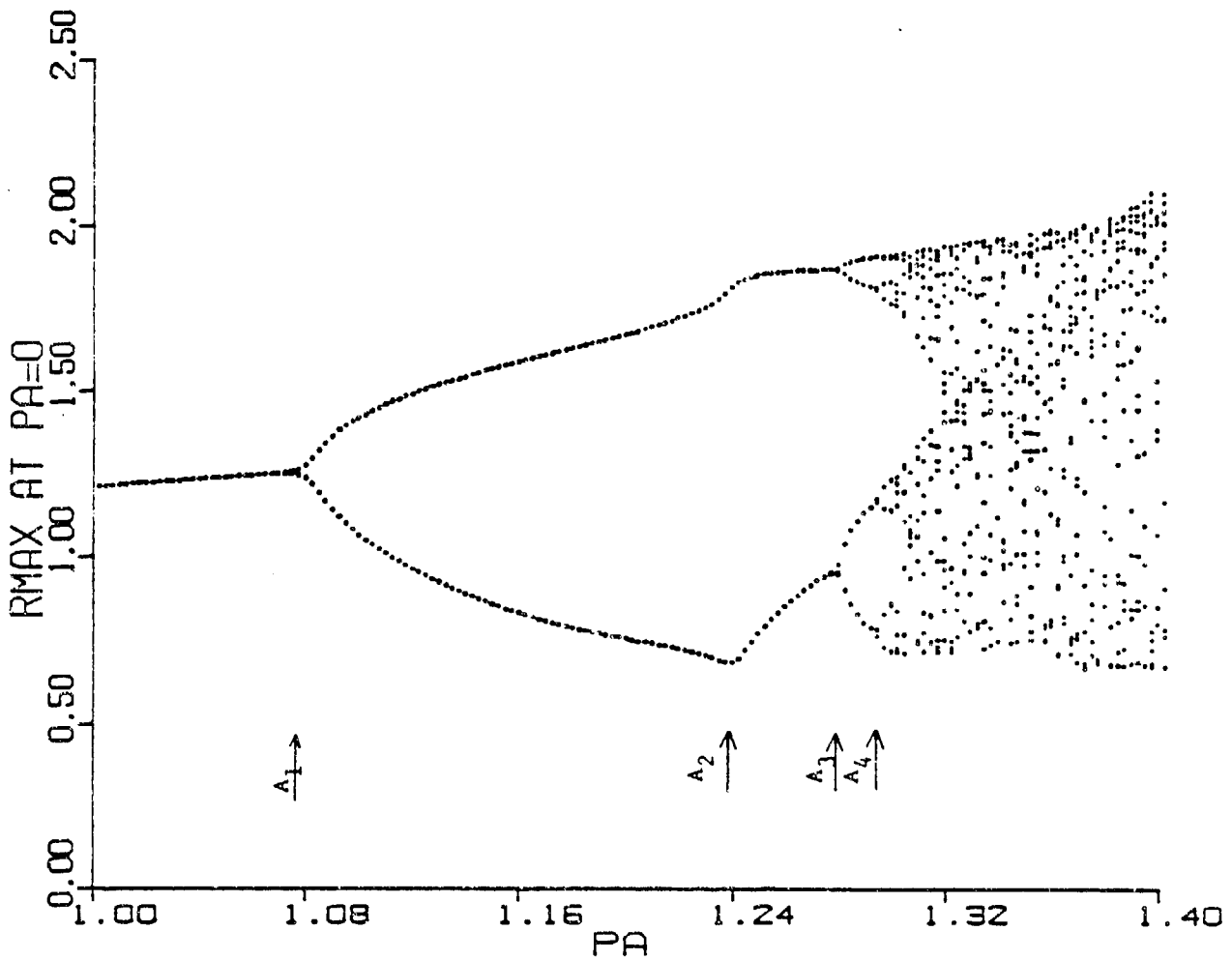

Fig. 24. Feigenbaum "tree" showing the systematic sequence of bifurcation leading to chaos for a gas bubble of 50 microns and driven at approximately one half its resonance frequency.

Thus, in principle, one can systematically determine the advent of each bifurcation and its associated frequency of sound radiation, as the system approaches chaos (or white noise).

What has all this to do with the biological effects of ultrasound? Quite a lot, really! The principal method used so far to determine that cavitation does or does not exist in an opaque medium is to detect the presence of radiated acoustic signals that are associated with cavitation - subharmonics or white noise. Our examination of where this noise originates, and why it is there is extremely important if these concepts are still to used said as cavitation indicators. Further, if clinical ultrasound systems are found to be inducing cavitation, either stable or transient, it will be very important to determine as much as we can about the nature of the cavitation and its potential for damage. We now examine a cavitation phenomenon that has high damage potential.

F. Sonoluminescence from stable cavitation

Sonoluminescence is a phenomenon first observed over 50 years ago [85] in which light is emitted from a gas bubble set into violent oscillation by an acoustic field. Several explanations [86] for this light emission have been given over the years but it is now reasonably well established [49-51] to be a result of the radiative recombination of certain free radical species produced by the collapsing bubble as it drives the interior gases to high temperatures.

Although detection schemes for this phenomenon have included the naked eye [87], exposure of photographic plates [88], and photomultipliers [88], recently Reynolds et.al. [89] have used an image intensification technique to record low-level emissions. We wish to now describe the use of this system to examine cavitation produced by an ultrasonic horn driver in a

tank of water. The horn produced standing waves within the tank and cavitation-like bubble activity was observed to occur at the pressure antinodes according to the general custom.

The experimental apparatus is shown in Fig. 25. After a desirable level of sonoluminscence was achieved by adjusting the position of the horn in the chamber, the output of the image intensifier tube (IIT) was recorded by a video camera on magnetic tape for a variety of voltages supplied to the horn. The patterns observed by the IIT were later reviewed with the VCR, and when a desirable feature was observed, the frame was frozen and a still photograph taken with a 35 mm camera. A succession of these photos for increasing pressure amplitude are shown in Fig. 26.

Fig. 26a shows that light emissions begin to appear in a layer near the tip of the horn. It is known that an antinodal plane of pressure should exist there and at successive half-wavelength distances from the horn in a vertical direction if standing waves are excited in the tank of water. In Fig. 26a the broad band of light emission near the bottom of the frame coincides with the horn tip. Note also that there is a single spot of light occurring in the upper left of this frame. This spot is at the position of the second antinodal plane as is indicated by the development of this band in Figs. 26b and 26c. The curious row of 6 separate spots of light in this band maintained their individual identities until the pressure amplitude was increased. As shown in Fig. 26d, a third row of individual light producing centers developed that became well defined in Fig. 26e. At this stage, there was considerable movement of the light emitting centers back and forth within separate antinodal planes, but no distinguishable movement between planes. Further, it is seen in Fig. 26e that the 6 separate centers of Fig. 26d have started to blend into one single band.

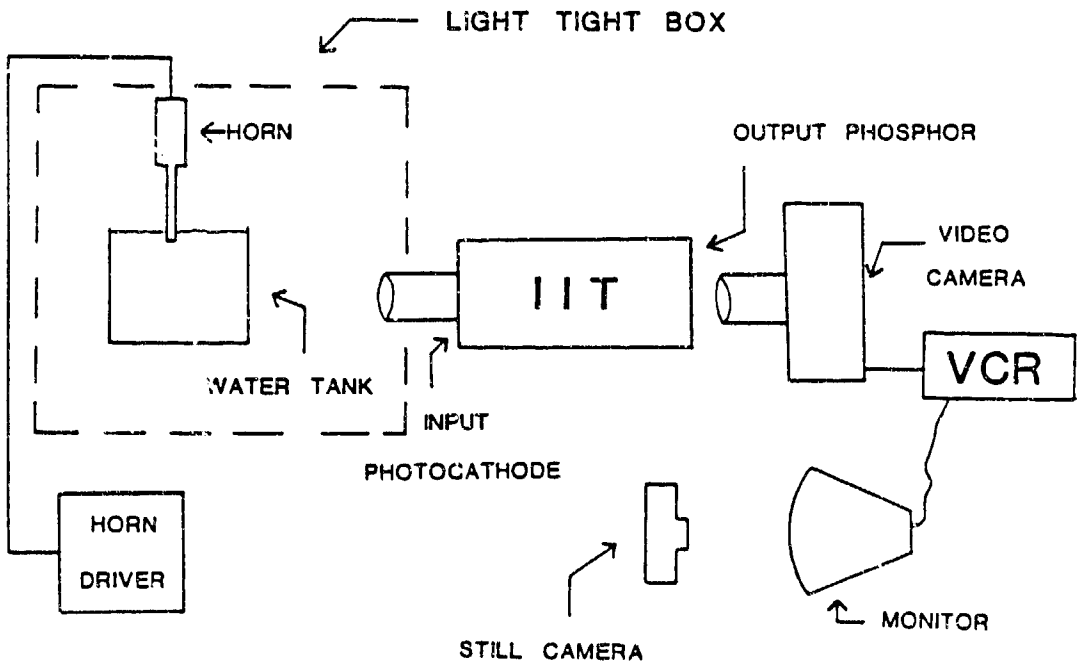

Fig. 25. Experimental arrangement for obtaining information about sonoluminescence using a image intensifier tube apparatus.

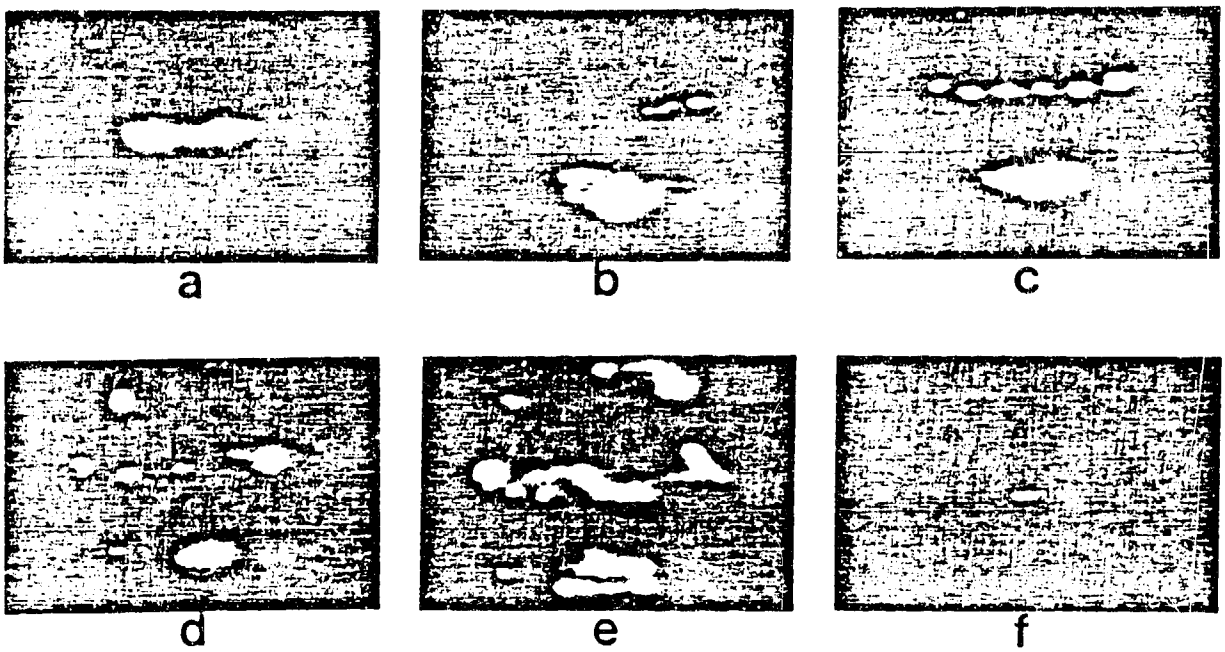

Fig. 26. Photographs taken from video monitor of sonoluminescence activity viewed by image intensifier tube for increasing levels of acoustic pressure amplitude. The horn is driven at its lowest level in (a) and at its highest level in (f), where the standing wave pattern is disrupted by violent cavitation on the horn tip. The "layers" of activity are due to bubbles trapped near antinodal planes separated by approximately a half wavelength.

If the pressure amplitude is increased even further, the light emission nearly ceases, except for one spot near the tip of the horn, as shown in Fig 26f. This effect is a well-known characteristic of cavitation produced by horn radiators and is a consequence of such violent cavitation on the horn tip that the sound is no longer propagated into the bulk of the fluid. A rough measurement of the sound field indicated a threshold for light emission on the order of 1.5 bars (0.15 MPa).

The degree of sonoluminescence activity described here is rather remarkable considering the relatively low level of cavitation activity associated with the modest levels of acoustic pressure amplitude generated in the tank.

A visual inspection of the system revealed that at low driving levels, say Fig. 26a, there was almost no bubble activity at all, perhaps a thin, barely visible "streamer", but certainly no "snappy" cavitation typical of transient events. Even at the highest level of light emission, as in Fig. 26e, only a few thin streamers were visible. On occasion, the feather-like track [90-92] and sharp snap of a transient event was observed, but only near the very bottom of the tank, well below the area viewed by the IIT. It appears that there can be considerable amounts of light emitted from what most of us would call "stable" cavitation.

In a detailed and extensive report on a similar experiment, Saksena and Nyborg [93] described the observation of sonoluminescence from "stable" cavitation in both water and a mixture of glycerine and water. There, light was observed even in the absence of streamers in the glycerine/water mixture. Our observations here corroborate those findings and indicate that violent, destructive collapses need not occur for considerable amounts of light output to occur. Since it is now rather well-established that the

light-emission mechanism is associated with free radical production (and recombination), the presence of sonoluminescence is an indication of potentially very harmful chemical activity.

Using our new formulation of bubble dynamics, we have been able to calculate the temperatures associated with a violently pulsating gas bubble driven near its principal resonance and at an off-resonance point. Shown in Fig. 27 is the temporal variation of the temperature for a 50 μm bubble driven at the modest pressure amplitude of 0.6 bar (0.06 MPa) and for frequencies equal to 0.8 and 0.4 times its resonance frequency. It can be seen that the temperature in the interior of the bubble rises to nearly 3000^{o}K, sufficiently high for luminescence to occur, for the excitation near the principal resonance.

G. Concluding remarks.

This phenomenon of stable cavitation becomes particularly appropriate, in a biological-effects sense, when one considers the fact that theraputic ultrasound with acoustic pressure amplitudes on the order of 0.1 MPa has been shown to induce bubble formation in vivo [25-26], and that these bubbles are made to grow by ultrasonic means [27]. A bubble trapped in tissue would not be as free to move away from the pressure maxima as they are in liquids, and accordingly could generate copious amounts of highly reactive free radicals. It seems logical that growth by rectified diffusion would also be restrained and consequently the bubble could spend a considerable number of oscillations in large-amplitude pulsation before it broke up, or grow through resonance by rectified diffusion. Further, even if it broke apart during its most violent oscillations, it would likely regrow through the large-amplitude regions again and again. It is not clear that these effects would always be harmful, especially since Dyson et.al. [75,94] have seen beneficial results, but with the widespread

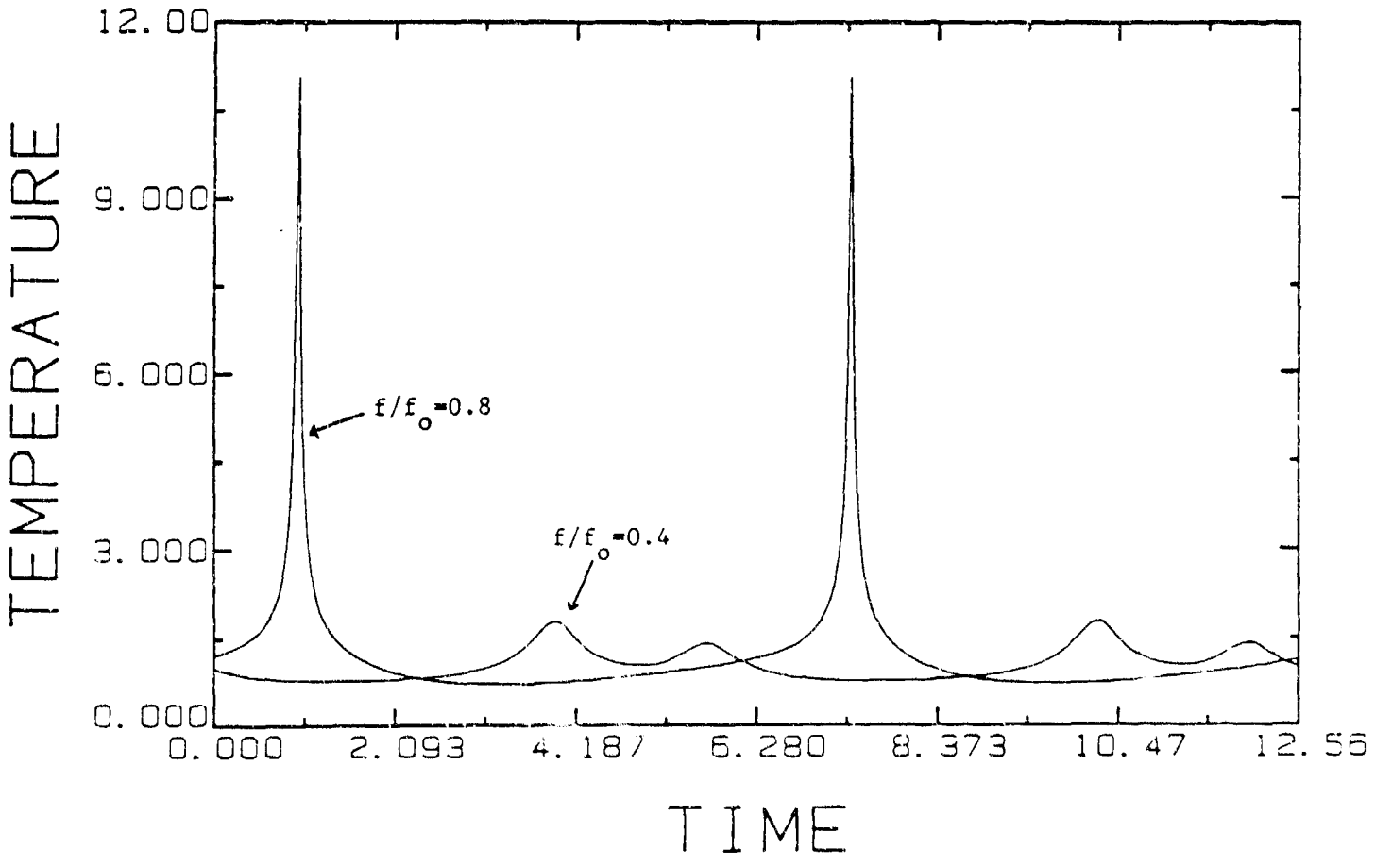

Fig. 27. Variation of the temperature inside a pulsating gas bubble as a function of time for different values of the driving frequency. For this case, the bubble radius was 50 microns and the acoustic pressure amplitude was 0.6 bars.

use of ultrasound systems in clinical medicine, increased attention should be given this phenomenon in order to ascertain what types of bio-effects may be occuring.

IV. EXPERIMENTAL MEASUREMENTS OF CAVITATION PRODUCED BY SHORT ACOUSTIC PULSES

In this section we wish to describe some recent experimental measurements that we have performed of cavitation produced by short acoustic pulses. We shall examine only the experimental aspects of the study; the theoretical analysis of short pulse cavitation is treated in another section by Professor Flynn.

A. Introduction

Recently Flynn [95] and Apfel [96] have calculated that microsecond length pulses of ultrasound can generate transient cavitation in water for temporal peak intensities in the range of 10 to 30 W/cm^2 (depending upon the initial conditions). Since some diagnostic ultrasound systems currently in clinical use generate microsecond length pulses with temporal peak intensities greater than 100 W/cm^2 [97-98], there was reason to believe that this mechanism could operate under diagnostic conditions in aqueous media. However, until this study, there had been no reported experimental confirmation of these theoretical calculations. We wish to present evidence that ultrasonic pulses as short as one cycle at a frequency of 1.0 MHz give rise to luminescence flashes characteristic of violent cavitation.

B. Experimental Procedure

The experimental system is described in more detail by Roy, et.al [99]; only a brief description will be given here.

Since the collapse of a cavitation "bubble" is restricted to extremely small dimensions at megahertz frequencies, we decided not to utilize the commonly used cavitation detection criterion -- the acoustic detection of a shock wave. There is incomplete evidence that cavitation collapses in this frequency regime will not be detectable acoustically. Rather, we have used

a photometric detection system based upon the observation, via a photomultiplier tube, that light is produced by the oxidation of luminol through a reaction that is initiated by the free radicals generated during the collapse of a cavity. We shall describe this process as chemiluminescence rather than sonoluminescence and discuss the distinction between the two processes later. The details of the experimental procedure are now given.

An essential ingredient of the cavitation generation system is that the acoustic pressure amplitude of the sound field is increased linearly with time, at a reproducible rate, until cavitation occurs. The heart of the system is a ramp generator that drives both the amplitude modulation input of a function generator and a strip recorder. The DC voltage level on the strip chart record is linearly related to the peak to peak output of the function generator. This signal is amplified and delivered to a focused transducer (resonance frequency approximately 1.0 MHz) that radiates into an echo-free chamber (walls lined with acoustic absorber) filled with distilled water containing luminol. The chart record is calibrated in units of megapascals by inserting a small, calibrated hydrophone (Medicoteknisk Institut, PVDF ultrasonic probe, o.d. 1.0mm) into the focal region of the sound field during simulated measurements at low amplitudes. Fig. 28 shows the cavitation generation apparatus that we use.

The cavitation detection scheme is critical to these measurements and is now described. Light generated by the collapsing cavity (discussed in more detail below) in the focal region is detected by a photomultiplier tube (PMT) and the resulting pulse from the PMT base is preamplified and fed into a pulse height discriminator. The discriminator level determines the sensitivity of the apparatus and is set to 600 mV, which is well above the average electrical background level (~150mV) but below the typical chemiluminescence pulse height (~1.0V). After discrimination, the signal

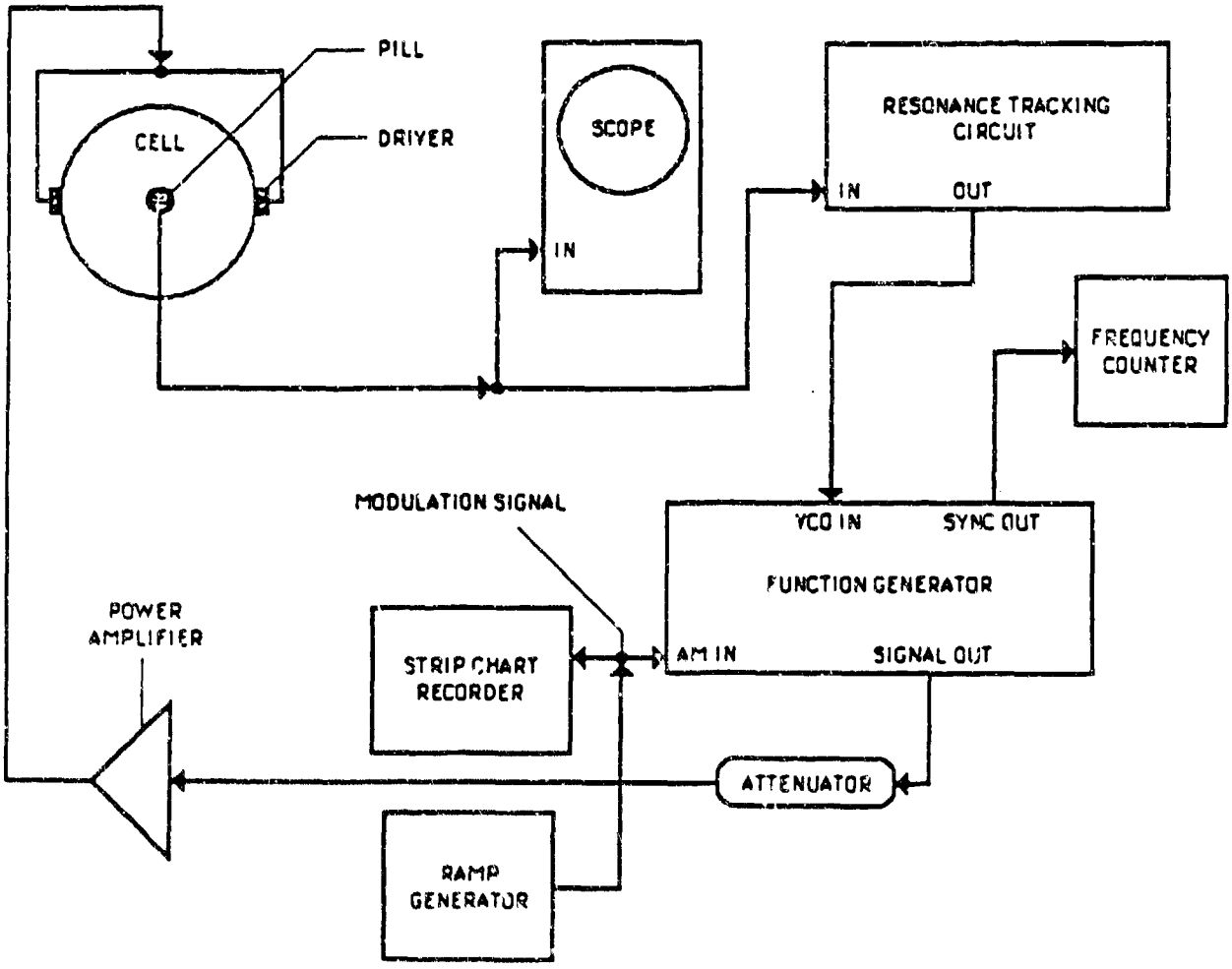

Fig. 28. Block diagram of cavitation generation apparatus for use in the study of cavitation produced by short acoustic pulses.

passes through a "noise gating" network that either ignores the signal (no decision) or resets the system (cavitation detected). The noise gating network is a type of "coincidence" counter that requires that two pulses are observed within a 100ms time interval. The reason for this cavitation detection criterion is that we have discovered through experience that a cavitation event typically generates several optical flashes during a 100ms interval while the background noise is randomly distributed in time. Thus, the coincidence requirement permits us to lower the "false count" rate to a small fraction of the total number of events. A "system reset" refers to an immediate reduction in the acoustic pressure amplitude to a quiescent level (zero amplitude) for a predetermined length of time and constitutes light detection. Fig. 29 shows the cavitation detection apparatus that we use.

The sequence of events that comprise a data run are then as follows: A timer disables the linear gate and the ramp generator for a fixed length of time, say 300 seconds. The linear gate prevents any stray noise pulses from resetting the timer before the quiescent period is over. At the end of this time, a slowly increasing voltage is supplied to the transducer, which simultaneously increases the acoustic pressure amplitude in the liquid. When the detection system observes more than two electrical pulses with heights greater than 600mV within the 100ms gate, the system (which includes the strip chart recorder) is reset to undergo another 300s quiescent time. This procedure is then repeated until a sufficient number of data points are collected. The chart recorder then provides a hard copy of the data generated.

We have taken measurements of the cavitation threshold as a function of pulse length and of length of time between pulses (duty cycle). A duty

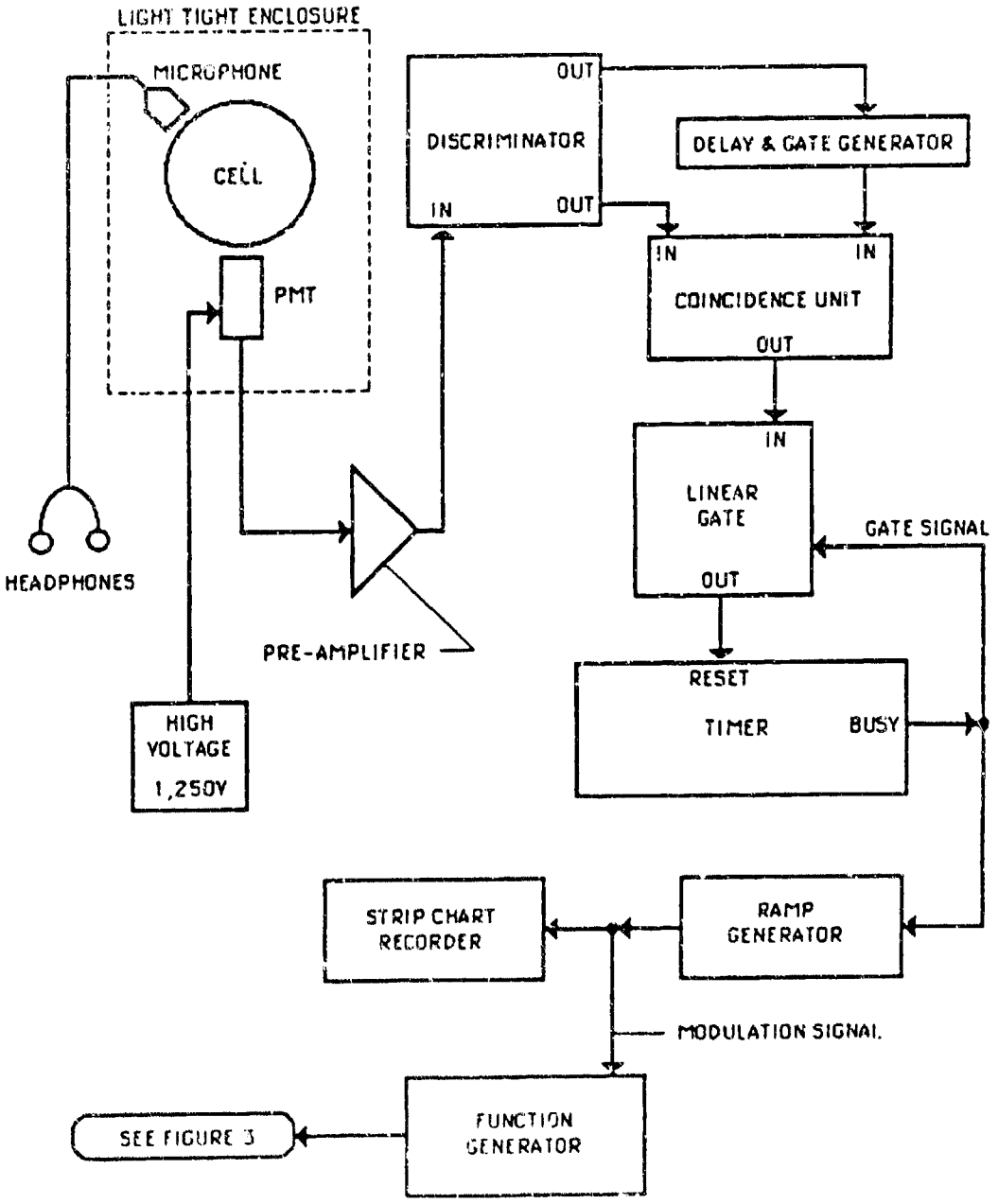

Fig. 29. Block diagram of cavitation detection apparatus for use in the study of cavitation produced by short acoustic pulses.

cycle of 1:10 means that the sound field is on for 1 time unit and off for the succeeding 9 time units.

C. Results

Figure 30 shows the measured values of the threshold acoustic pressure amplitude required to trigger a system reset as a function of pulse length for distilled water containing luminol. The data presented here are for a duty cycle of 1:10; similar behavior is observed for duty cycles of 1:3, 1:5 and 1:20. The values of the temporal peak acoustic pressure are given because it is this parameter that is important in the generation of cavitation effects, not the average intensity [100]. An approximate value of the temporal peak intensity can be obtained by assuming a plane wave and using the relation $I = P_a^2/2\rho c$, where P_a is the temporal peak acoustic pressure, ρ is the density of the liquid and c the velocity of sound in the liquid. Values of the intensity reported in this paper will be calculated using the above relationship between intensity and pressure. We have plotted the "cavitation threshold" as a function of the logarithm of the pulse length to compress the scale. Since the frequency used was 1.0 MHz, an abscissa value of 3 implies that about 1000 cycles were contained in the pulse, 2 means 100, 1 means 10 and 0 indicates that the pulse contained essentially one cycle.

Each data point presented is the average of at least 10 individual measurements; the error bars represent $\pm$ one standard deviation from the mean. For the critical data point at an abscissa value of 0 -- one acoustic cycle -- we have taken over 30 separate measurements on three different days with three different liquid samples. On one occasion a second operator made the measurements (although the system is essentially automated). Furthermore, at a duty cycle of 1:10, and at values of the temporal peak acoustic pressure only slightly higher than that determined as the "thresh-

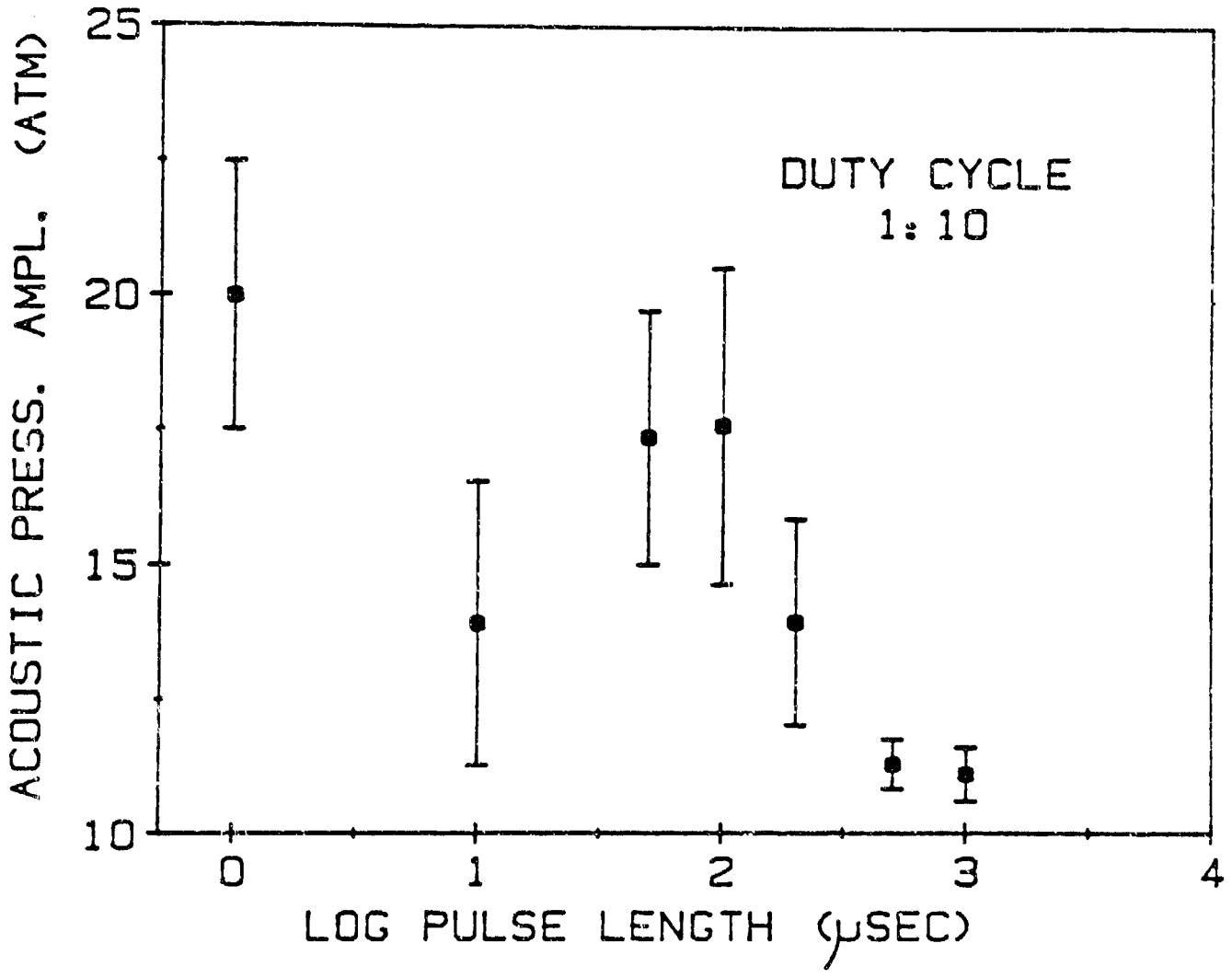

Fig. 30. Variation of the acoustic cavitation threshold of water containing luminol with pulse length for a duty cycle of 1:10. The points are the average of at least 10 independent measurements and the error bars represent ± one standard deviation. The carrier frequency was 1.0 MHz and the liquid was saturated with argon.

old", single cycle pulses of 1 MHz ultrasound give light emission that is visible to the naked eye.

Figure 31a shows a photo of the electrical pulse supplied to the transducer, and 31b the temporal variation of the acoustic pressure as measured by our miniature probe hydrophone. Note that there is some ringing of the transducer but only at a much reduced amplitude.

We have also examined the dependence of the "cavitation threshold" on duty cycle for the "one-cycle" pulse. These data are shown in Fig. 32. We have been concerned that the cavitation nuclei may respond to the pulse repetition frequency rather than the individual pulses. These data have greatly reduced that concern.

There are several important aspects of these data that need to be addressed.

First of all, we have established an arbitrary definition of the threshold. By our definition, the cavitation threshold is that value of the peak temporal acoustic pressure at which PMT output pulses reaching the pulse height discriminator have values of 600 mV or larger. This requirement is a working definition in that this discriminator setting permits us to obtain a desirable signal-to-noise ratio. It is quite conceivable that a more sensitive detection system would indicate lower values of the threshold (see the discussion of the meaning of threshold for this system as described in ref. [99]). We are currently attempting to acquire a more sensitive system to determine if the values of the threshold obtained in this study can be significantly lowered.

Second, we have used a definition of cavitation that involves the production of light by the collapsing cavity. Sonoluminescence is a reasonably well-understood phenomenon [86] that is apparently the result of

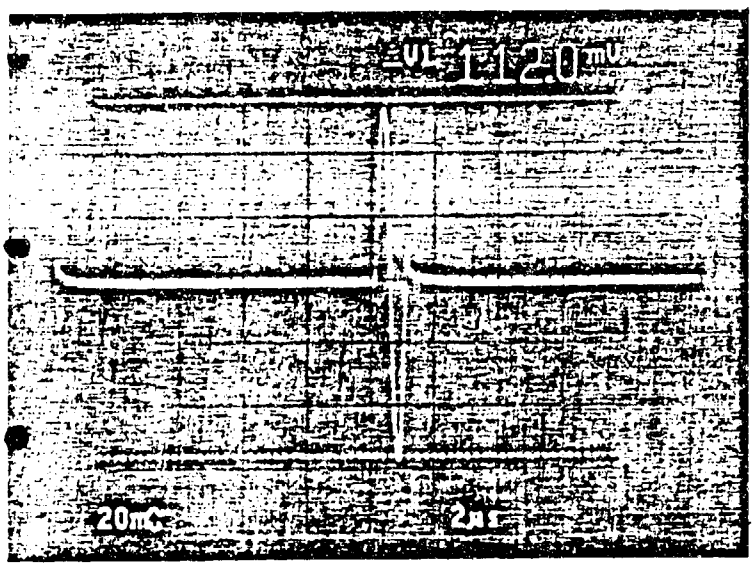

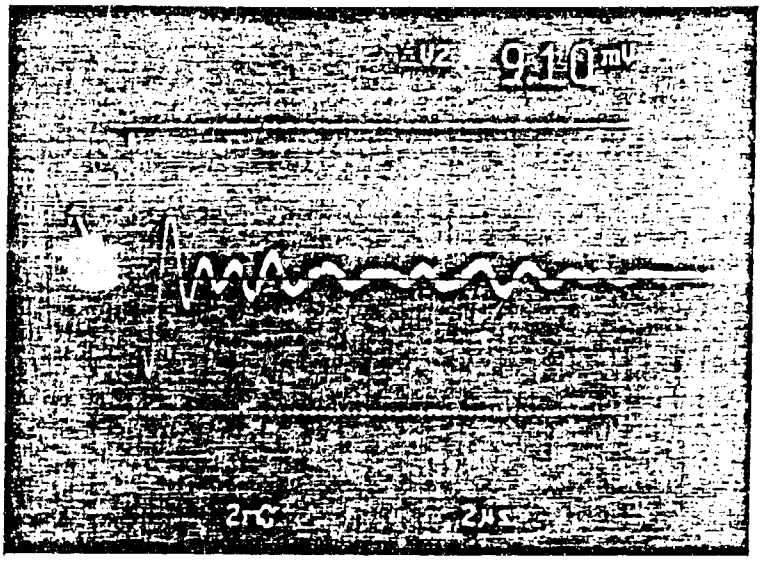

Fig. 31. (a) The electrical signal supplied to the transducer for single-cycle pulses. (b) The temporal variation of the acoustic pressure near the focus of the sound field as measured by a calibrated miniature hydrophone for the electrical signal in (a).

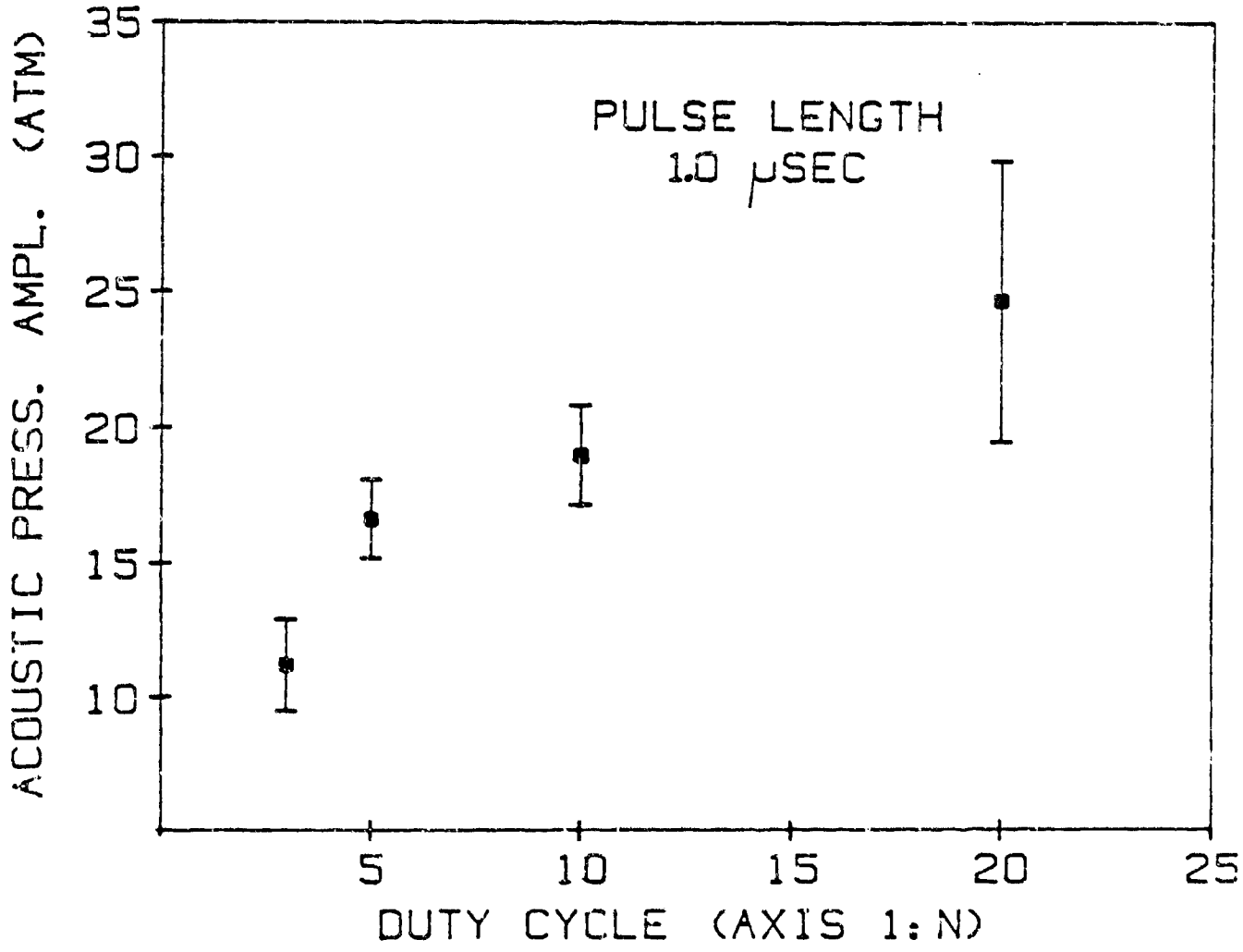

Fig. 32. Variation of the acoustic cavitation threshold of water containing luminol with duty cycle for a pulse length of approximately 1 microsecond. The carrier frequency was 1.0 MHz and the liquid was saturated with argon.

the radiative recombination of free radicals produced by the high temperatures and pressures developed by the collapsing cavity [49-51]. However, the light emission that we observe is probably not sonoluminescence produced by the recombination of free radicals within the cavity itself. Rather, we observe light from the bulk of the liquid indirectly resulting from free radicals produced within the cavity. Luminol has been used by several researchers (see for example, ref. [88]) to increase the output of light emissions from acoustic cavitation and the specific oxidation reactions that lead to light emission have been studied in some detail [101-102]. What is most important, and relevant to this work is that the presence of free radicals are required for light emission to occur. Since these free radicals are highly reactive, and pose a threat to biological tissues, it is their presence that is important, not the light emission per se.

A third aspect of the observation reported here is that the light emission from the insonified area can be seen by the naked eye, and appears in the form of "streaks" rather than "flashes". We interpret this phenomenon to be due to the relatively long lifetime of the oxidation reaction (as long as 50ms according to Finch [88]) and the rapid movement of collapsing cavities through the focal region due to radiation pressure forces. However, as discussed earlier, we have also recently observed intense light emission from a form of "stable" cavitation with the use of an image intensifier tube as a light detector [103]. Although the temporal peak acoustic pressures are quite large, we don't wish to discount some form of stable cavitation at this time, especially since the liquid probably contains a large number of large cavitation nuclei [104].

D. Some Final Concluding Comments

Our recent examination of the possible generation of cavitation by

clinical devices has lead us to the following conclusions.

(i) There can be no doubt that small pockets of free gas are contained in biological tissue; the widespread presence of these microbubbles is well established by decompression studies.

(ii) It has been observed experimentally that these microbubbles can be activated by both continuous and pulsed acoustic systems. Furthermore, the experimental oservations are roughly in agreement with the theoretical pedictions.

(iii) Because cavitation is hard to detect, unless one knows what to look for, there is now <u>good reason to believe</u> that cavitation is being produced by some therapeutic and diagnostic ultrasound devices. An extensive risk-assessment study emphasizing the <u>physical mechanisms</u> should be carried out immediately.

V. LIST OF REFERENCES

[1]. R.E. Apfel, Nature 223, 119 (1971).

[2]. R. Roy, A. Atchley, L. Crum, J. Fowlkes and J. Reidy, "A precise technique for the measurement of acoustic cavitation thresholds, and some preliminary results", J. Acoust. Soc. Am. (to be published).

[3]. P.S. Epstein and M.S. Plesset, J. Chem. Phys. 18, 1505 (1950).

[4]. T. Alty, Proc. Roy. Soc. Ser. A. 112, 235 (1926).

[5]. M.G. Sirotyuk, Sov. Phys. Acoust. 16, 482 (1971).

[6]. V.A. Akulichev, Sov. Phys. Acoust. 12, 144 (1966).

[7]. F.E. Fox and K.F. Herzfeld, J. Acoust. Soc. Am. 26, 985 (1954).

[8]. M. Strasberg, J. Acoust. Soc. Am. 31, 163 (1959).

[9]. K.F. Herzfeld, Comment in Proc. First Sympos. Naval Hydrodyn. (Nat. Acad. Sci., Wash. D.C.), F.S. Sherman, ed. pp. 319-320 (1957).

[10]. M.G. Sirotyuk, Sov. Phys. Acoust. 16, 237 (1970).

[11]. D.E. Yount and R.H. Strauss, J. Appl. Phys. 47, 5081 (1976).

[12]. D.E. Yount, J. Acoust. Soc. Am. 65, 1429 (1979).

[13]. D.E. Yount, C.M. Yeung, and F.W. Ingle, J. Acoust. Soc. Am. 65, 1440 (1979).

[14.] D.E. Yount, J. Acoust. Soc. Am. 71, 1473 (1982).

[15]. D.E. Yount, E.W. Gillary and D.C. Hoffman, J. Acoust. Soc. Am. 76, 1511 (1984).

[16]. A.A. Atchley, "The nucleation of cavitation in aqueous media", Ph. D. Dissertation, University of Mississippi, Oxford, MS (1985).

[17]. E.N. Harvey, K.K. Barnes, W.D. McElroy, A.H. Whitely, D.C. Pease and K.W. Cooper, J. Cell. Comp. Physiol. 24, 1 (1944).

[18]. R.E. Apfel, J. Acoust. Soc. Am. 48, 1179 (1970).

[19]. L. A. Crum, Nature 218, 148 (1979).

[20]. L.A. Crum, "Acoustic Cavitation Thresholds in Water", in Cavitation and Inhomogeneities in Underwater Acoustics, W. Lauterborn, ed., (New York, Springer-Verlag) 1980.

[21]. A.A. Atchley and A. Prosperetti, "The critical radius approach to the crevice model of cavitation nucleation", J. Acoust. Soc. Am. (to be published).

[22]. F.G. Blake, "The onset of cavitation in liquids", Tech. Memo. No. 12, Acoustics Research Lab. Harvard University, (1949).

[23]. A. Prosperetti, "Bubble phenomena in sound fields", Ultrasonics (to be published).

[24.] W. Galloway, J. Acoust. Soc. Am. 26, 849 (1954).

[25.] G. ter Haar and S. Daniels, Phys. in Med. Biol. 26, 1145 (1981).

[26]. G. ter Haar, S. Daniels, S. Eastaugh and C.R. Hill, Dr J. Cancer, 45, 151 (1982).

[27]. L.A. Crum and G.M. Hansen, Phys. Med. and Biol. 27, 413 (1982).

[28]. S.Z. Child and E.L. Carstensen, Ultrasound Med. Biol. 8, 311 (1982).

[29]. S.Z. Child, E.L. Carstensen and S.K. Lam, Ultrasound Med. Biol. 7, 167 (1981).

[30]. P.M. McDonough and E.A. Hemmingsen, J. Appl. Physiol. 56, 513 (1984).

[31]. P.M. McDonough and E.A. Hemmingsen, J. App.Physiol. 57, 117 (1984).

[32]. L.A. Frizzell, C.S. Lee, P.D. Aschenback, M.J. Borrelli, R.S. Morimoto, and F. Dunn, J. Acoust. Soc. Am. 74, 1062 (1983).

[33]. W.D. Fraser, J.P. Landolt and K.E. Monev, Acta Otolaryngol 95, 95 (1983).

[34]. H.D. Van Liew, Am. J. Physiol. 214, 1176 (1968).

[35]. H.D. Van Liew and M Passke, Aerosp. Med. 38, 829 (1967).

[36]. E.A. Hemmingsen, J. Exp. Zool. 220, 43 (1982).

[37]. F.C. Golding, P. Criffiths, W.D.M. Paton, D.N. WAlder, and H.V. Hempleman, Br. J. Ind. Med. 17, 167 (1960).

[38]. O.E. Van Der Aue, R.J. Keller and E.S. Brinton, "The effect of exercise during decompression from increased barometric pressures on the incidence of decompression sickness in man", Washington D.C. US Navy Exp. Diving Unit, 1949. (Res. Rept. 8-49).

[39]. C.G. MacKenzie and A.H. Reisen, J. Am. Med. Assoc. 124, 499 (1944).

[40]. M.P. Spencer, D.C. Johnson and S.D. Campbell, "Safe decompression with the Doppler ultrasonic blood bubble detector" in Underwater Physiology V, C.J. Lamberten, ed. (Bethesda, MD: FASEB), 1976, pp. 311-325.

[41]. J.A. Rooney, J. Acoust. Soc. Am. 52, 1718 (1972).

[42]. P.A. Lewin and L. Bjorno, J. Acoust. Soc. Am. 71, 728 (1982).

[43]. P.A. Lewin and L. Bjorno, J. Acoust. Soc. Am. 69, 864 (1981).

[44]. D.L. Miller, Ultrasound Med. Biol. 5, 351 (1979).

[45]. A.R. Williams and D.L. Miller, Ultrasound Med. Biol. 6, 251 (1980).

[46]. C.L. Kling and F.G. Hammitt, J. Basic Engr. D94, 825 (1972).

[47]. C.F. Naude and A.T. Ellis, J. Basic Engr. 83, 648 (1961).

[48]. W. Lauterborn, Appl. Phys. Lett. 21, 27 (1972).

[49]. C. Sehgal, R. G. Sutherland and R. E. Verrall, J. Phys. Chem. 84, 2920 (1980).

[50]. C. Sehgal, R. G. Sutherland and R. E. Vervall, J. Phys. Chem. 70, 2242 (1979).

[51]. C. Sehgal, R. G. Sutherland and R. E. Verrall, J. Phys. Chem. 84, 529 (1980).

[52]. P. Riesz, D. Berdahl, and C.L. Christman, "Free radical generation

by ultrasound in aqueous and non-aqueous solutions", Environmental Health Persectives (to be published).

[53]. D.Y. Hsieh and M.D. Plesset, J. Acoust. Soc. Am. 33, 206 (1961).

[54]. M. Strasberg, J. Acoust. Soc. Am. 33, 359 (1961).

[55]. A.I. Eller and H.G. Flynn, J. Acoust. Soc. Am. 37, 493 (1965).

[56]. M.H. Safar, J. Acoust. Soc. Am. 43, 1188 (1968).

[57]. A.I. Eller, J. Acoust. Soc. Am. 46, 1246 (1969).

[58]. R.K. Gould, J. Acoust. Soc. Am. 56, 1740 (1974).

[59]. B.J. Davison, J. Sound Vib. 17, 261 (1971).

[60]. O.A. Kapustina and Y.G. Statmikov, Sov. Phys. Acoust. 13, 327 (1968).

[61]. L.A. Skinner, J. Acoust. Soc. Am. 51, 378 (1972).

[62]. A.I. Eller, J. Acoust. Soc. Am. 57, 1374 (1975).

[63]. L.A. Crum, J. Acoust. Soc. Am. 68, 203 (1980).

[64]. R.E. Apfel, J. Acoust. Soc. Am. 64, 1624 (1981).

[65]. L.A. Crum and G.M. Hansen, Phys. Med. Biol. 27 413 (1982).

[66]. L.A. Crum, Ultrasonics, 22, 215 (1984).

[67]. A. Prosperetti, J. Acoust. Soc. Am. 61, 17 (1977).

[68]. A.E. Eller, J. Acoust. Soc. Am. 47, 1469 (1970).

[69]. C. Devin, J. Acoust. Soc. Am. 31, 1654 (1959).

[70]. A.S. Tucker and C.A. Ward, J. Appl. Phys. 46, 4801 (1975).

[71]. V.F.K. Bjerknes, Die Kraftfelder (Vieweg and Sohn, Braunschweig, Germany, 1909).

[72]. L. A. Crum, J. Acoust. Soc. Am. 57, 1363 (1975).

[73]. L.A. Crum and G.M. Hansen, J. Acoust. Soc. Am. 72, 1586 (1982).

[74]. A. Prosperetti, J. Acoust. Soc. Am. 56, 878 (1974).

[75]. M. Dyson, Infections in Surgery, 9, 37 (1982).

[76]. A. Prosperetti, Ultrasonics, 22, 77 (1984).

[77]. J.B. Keller and M. Miksis, J. Acoust. Soc. Am. 68, 628 (1980).

[78]. L.A. Crum, J. Acoust. Soc. Am. 73, 116 (1983).

[79]. W. Lauterborn, J. Acoust. Soc. Am. 69, 1624 (1981).

[80]. L.A. Crum and A. Prosperetti, J. Acoust. Soc. Am. 73, 121 (1983).

[81]. L. A. Crum and A. Prosperetti, J. Acoust. Soc. Am. 75, 1910 (1984).

[82]. A. Prosperetti, L. A. Crum and K. C. Commander, J. Acoust. Soc. Am. (to be published).

[83]. W. Lauterborn and E. Cramer, Phys. Rev. Lett. 47, 1445 (1981).

[84]. M.J. Feigenbaum, J. Stat. Phys. 19, 25 (1978).

[85]. N. Marinesco and J.J. Trillat, C.r. Lebd. Seanc. Acad. Sci., Paris, 196, 858 (1933).

[86]. A.J. Walton and G.T. Reynolds, "Sonoluminescence", submitted to Advances in Physics.

[87]. L.A. Chambers, J. Chem. Phys. 5, 280 (1937).

[88]. R.D. Finch, Ultrasonics 1, 87 (1964).

[89]. G.T. Reynolds, A.J. Walton and S. Gruner, Rev. Sci. Inst. 53, 1673 (1982).

[90]. G.W. Willard, J. Acoust. Soc. Am. 25, 669 (1953).

[91]. E.A. Neppiras and W.T. Coakley, J. Sound Vib. 45, 341 (1976).

[92]. L.A. Crum and D.A. Nordling, J.Acoust. Soc. Am. 52, 294 (1972).

[93]. T.K. Saksena and W.L. Nyborg, J.Chem. Phys. 53, 1722 (1970).

[94]. M.Dyson and D.S. Smalley, in ultrasound Interactions in Biology and Medicine, R. Millner, E. Rosenfeld and V. Cobet, eds. (Plenum:London) 1983.

[95]. H.G. Flynn, J. Acoust. Soc. Am. 72, 1926 (1982).

[96]. R.E. Apfel, Brit. J. Cancer, Suppl. V, 45, 140 (1982).

[97]. E.L. Carstensen and H.G.Flynn, Ultrasound Med. Biol.8, L720 (1982).

[98]. F.W. Kremkau, Clinics in Obstet. Gyn. 10, 395 (1983).

[99]. R.A.Roy, A.A.Atchley, L.A. Crum, J.B.Fowlkes, and J.J. Reidy, "A precise technique for the measurement of acoustic cavitation tnresholds, and some preliminary results", J. Acoust. Soc. Am. (to be published).

[100]. E.L. Carstensen, K.J. Parker and D. B. Barbee, J. Acoust. Soc. Am. 74, 1057 (1983).

[101]. E. H. White and D. F. Roswele, Acc. Chem. Res. 3, 54 (1970).

[102]. T.G. Burdo and W.R. Seitz, Anal. Chem. 47, 1643 (1975).

[103]. L. A. Crum and G. T. Reynolds, "Sonoluminescence from stable cavitation", J. Acoust. Sc. Am. (to be published).

[104]. L.A. Crum, App. Sci. Res. 38, 101 (1982).

[105]. W. Connolly and F. Fox, J. Acoust. Soc. Am. 26, 843 (1954).